



Cholera dynamics driven by human behavior change via a degenerate reaction-diffusion model

Wenjing Wu, Qianying Zhang, Hao Wang and Shengqiang Liu

Abstract. Cholera remains a considerable public health challenge globally, especially in regions with inadequate water infrastructure. During disease outbreaks, human behavior changes often serve as a critical, and sometimes primary, factor influencing disease transmission. This paper proposes a degenerate reaction-diffusion model that incorporates distinct human mobilities and human behavior change under a spatially heterogeneous environment to investigate the dynamics and mitigation of cholera outbreaks. A key index, the basic reproduction number, is introduced as a surrogate for infection risk, providing insights into the potential for extinction or persistence of cholera. The asymptotic profiles of positive steady states are explored as human mobility to zero or infinity. Specifically, positive human behavior changes may reduce the asymptotic profiles under certain conditions. Numerical simulations are employed to examine how heterogeneity, human mobility and human behavior change influence infection risk and final epidemic size. Our findings indicate that infection risk alone is insufficient for predicting final epidemic size. While human behavior changes do not fundamentally alter the infection risk, they may quantitatively reduce the final epidemic size, thereby regulating the spread of cholera. The methods and results presented in this study can be applied to investigate other host-pathogen models.

Mathematics Subject Classification. 35K57, 35J57, 35B40, 92B05 .

Keywords. Cholera, Reaction-diffusion system, Spatial heterogeneity, Human behavior change, Asymptotic profiles.

1. Introduction

Cholera is an acute gastrointestinal epidemic caused by the bacterium *Vibrio cholerae* (or *V. cholerae*) [1], which produces toxins and thrives in brackish aquatic environments. The disease presents a significant public health threat, particularly in regions with limited access to safe drinking water and healthcare resources [2], and is characterized by severe symptoms including watery diarrhea, vomiting, thirst, abdominal pain, kidney failure, and low blood pressure, potentially resulting in death if left untreated. The infection process of cholera is influenced by complex interactions among human body, *V. cholerae*, and environment [1]. Transmission can occur both indirectly, through contaminated food or water [3–6], and directly, via contact with infected individuals [7–9]. Historically, cholera has caused seven documented pandemics and numerous localized outbreaks. Notably, the Yemeni cholera outbreak stands as the most extensive recorded event in recent times, resulting in over 2800 fatalities [10] and an estimated 2.5 million cases as of November 2021 [11].

Mathematical modeling plays a crucial role in understanding the mechanisms of cholera spread, building upon the Cappasso-Fontona model [13] and the Codeço model [12]. One approach, as employed by [7, 8, 13], involves classifying individuals and pathogens into distinct compartments. According to the fact that infections will manifest when bacterial density surpasses a specified threshold, Kong et al. [4] conducted an iSIR model which incorporates the susceptible-infected-recovered model along with indirect transmission. Actually, the classification of subpopulations is associated with disease-related factors such as transmission mode, recovery, and hyper-infectivity, as well as ecological, geographical, socio-economic,

population, mobility, and demographic factors [14]. Spatial heterogeneity is crucial in epidemiological models [15] and natural ecosystems [16]. Consequently, it is natural to construct epidemic models with transmission coefficients that depend on the spatial location of contact. Indeed, human mobility can exert influence on both infection risk and the final epidemic size [17]. To capture the complex influence of spatial heterogeneity and human mobility on the dynamics of cholera, researchers have commonly employed reaction-diffusion equations [18–22].

There is a mutual interaction between epidemics and human behaviors. Human behavior plays a crucial role in reducing morbidity and mortality by decreasing exposure to infectious agents and influencing epidemic and endemic patterns. Conversely, epidemic outbreaks may increase awareness of the potential for infection, leading to changes in population activities and social behaviors [23–25]. For cholera, individuals aware of the transmission risk may prioritize personal hygiene and sanitation measures, such as frequent handwashing, proper waste disposal, water sterilization, and vaccination or antibiotic prophylaxis [11, 26, 27]. Recently, a few mathematical models have addressed human behavioral aspects associated with cholera [28–33]. Wang et al. [28] integrated human behavior changes into a cholera model, demonstrating that positive human behavior changes can mitigate infection risk, size, magnitude, and spatial dispersal velocity of cholera. Al-Arydah et al. [29] showed that disease education proved more effective than water chlorination in reducing cholera transmission. To our knowledge, few studies have simultaneously considered human behavior change and spatial heterogeneity in cholera dynamics, except for a few recent works [19, 20, 33]. Nevertheless, existing models fall short in presenting the asymptotic profiles of the positive steady state (PSS) and the basic reproduction number (\mathfrak{R}_0) under different dispersal rates, and do not incorporate numerical simulations to evaluate the effect of spatial heterogeneity, human mobility and human behavior change on the final epidemic size.

This paper explores the roles of spatial heterogeneity, distinct human mobilities and human behavior change in the cholera dynamics via a degenerate reaction-diffusion model. Our research is motivated by previous works [18, 22, 34, 35], and aims to address the following objectives:

- (i) The introduction of a degenerate reaction-diffusion model for cholera, where the transmission rate and shedding rate of pathogen depend on the density of the infected individuals, entails the establishment of the well-posedness of the model, particularly in light of distinct dispersal rates. Moreover, demonstrating the existence of a global attractor involves tackling difficulties associated with the ordinary differential equation presented in the model.
- (ii) The basic reproduction number, denoted \mathfrak{R}_0 , is defined and analyzed for its monotonic dependence on dispersal rates, coefficients related to indirect contact, and shedding rates. However, \mathfrak{R}_0 is independent of the coefficients associated with human behavior change. We derive cholera extinction or persistence based on \mathfrak{R}_0 : the infection-free steady state (IFSS) is globally asymptotically stable when $\mathfrak{R}_0 < 1$, while the system exhibits uniform persistence when $\mathfrak{R}_0 > 1$.
- (iii) We investigate the asymptotic profiles of positive steady states (PSS) and \mathfrak{R}_0 as small or large dispersal coefficients of susceptible individuals. The results provide deeper insights into the structure of \mathfrak{R}_0 and PSS, indicating that significant human behavior changes and prompt response rates of media and individuals may mitigate certain asymptotic profiles of PSS. To our knowledge, this result provides the first theoretical evidence that positive human behavior changes may reduce the final asymptotic profiles of PSS under certain conditions.
- (iv) Numerical simulations are employed to validate and supplement the theoretical conclusions. The simulations demonstrate that mitigating spatial heterogeneity may effectively regulate the transmission of cholera; Augmenting the mobility of infected individuals has the potential to diminish the final epidemic size, while the optimal dispersal rate of susceptible individuals exists within an intermediate range; Infection risk alone is insufficient for predicting the final epidemic size; Human behavior change can significantly mitigate the final epidemic size.

This paper is structured as follows. Section 2 introduces a degenerate reaction-diffusion cholera model that integrates considerations of human behavior change and spatial heterogeneity. Section 3 obtains the

well-posedness of the cholera model, encompassing uniqueness, global existence, and boundedness of the solution, and demonstrates the existence of a global attractor. Section 4 defines \mathfrak{R}_0 , and employs it to obtain the threshold dynamics. Section 5 discusses the asymptotic profiles of \mathfrak{R}_0 and PSS for small or large dispersal coefficients. Section 6 provides numerical simulations to support and expand the theoretical conclusions. Finally, a discussion concludes the paper.

2. The model

In this section, a degenerate reaction-diffusion model is formulated to delineate the dynamics of cholera transmission. Pathogens in contaminated water are integrated into a disease model to establish a host-pathogen model. Inspired by host-pathogen models [18, 36–38], we hypothesize that individuals are mobile only in habitat, and the *V. cholerae* is constrained within the polluted water environment in habitat, i.e., *V. cholerae* is immobile. Actually, public health officials may opt for isolation of infected individuals to mitigate the outbreaks of disease [17]. Consequently, the mobility of susceptible individuals differ from those of infected individuals. The typical duration of cholera immunity spans approximately three to five years [39, 40], and we consider the situation that recovered individuals do not experience loss of immunity during the initial phase of an outbreak (within the first 12 months). Due to the fact that human behavior change exerts an influence on the density of the fresh infections individuals and *V. cholerae* [19], the contact rate and shedding rate of individuals are related to disease prevalence, location, and time. In order to make things less complex (since non-uniformness of dispersal rates, spatial heterogeneity and human behavior change have already made the issue extremely challengeable), we make a small concession in the interaction term by ignoring human-to-human (direct) infection route. With these consideration, we propose a hybrid model of two PDEs coupled with one ODE:

$$\begin{cases} \frac{\partial S}{\partial t} = D_S \Delta S + \Lambda(x) - \beta_1(I, x)SB - d_1(x)S, \\ \frac{\partial I}{\partial t} = D_I \Delta I + \beta_1(I, x)SB - (\gamma(x) + d_2(x) + d_3(x))I, \\ \frac{\partial B}{\partial t} = \beta_2(I, x)I - \delta(x)B \end{cases} \quad (2.1)$$

for $(x, t) \in \Omega \times (0, \infty)$, with the initial condition

$$S(x, 0) = S_0(x) \geq 0, \quad I(x, 0) = I_0(x) \geq 0, \quad B(x, 0) = B_0(x) \geq 0, \quad x \in \Omega \quad (2.2)$$

and homogeneous Neumann boundary conditions

$$\frac{\partial S}{\partial \vartheta} = \frac{\partial I}{\partial \vartheta} = 0, \quad (x, t) \in \partial\Omega \times (0, \infty). \quad (2.3)$$

Here $\Omega \subset \mathbb{R}^n$, $n \geq 1$ represents a bounded spatial habitat with sufficiently smooth boundary $\partial\Omega$. Let $S = S(x, t)$ and $I = I(x, t)$ describe the population densities of susceptible and infected individuals at location x and time t , respectively. Denote $B = B(x, t)$ as the density of *V. cholerae* in the polluted water at location x and time t . Constants $D_S > 0$ and $D_I > 0$ denote the dispersal rates of S and I , separately. The parameter $\Lambda(x)$ describes the influx rate of susceptible individuals, $d_1(x)$, $d_2(x)$ and $\delta(x)$ stand for the rates of natural mortality of susceptible individuals, infected individuals and *V. cholerae*, respectively. Let $\gamma(x)$ be the rate at which infected individuals recover, $d_3(x)$ describes the disease-related death rate of infected individuals. The functions $\beta_1(I, x)$ and $\beta_2(I, x)$ denote transmission rates from *V. cholerae* to susceptible individuals and shedding rate of pathogen by infected individuals, respectively. The boundary condition implies that no net mobility of individuals crosses the boundary $\partial\Omega$ with $\frac{\partial}{\partial \vartheta}$

being the derivative in the direction of the unit outward normal ν . More precisely, we assume

$$\beta_i(I, x) = \left(a_i - b_i \frac{I}{I + M_i} \right) \hat{\beta}_i(x), \quad i = 1, 2,$$

where a_1 (resp. a_2) represents the indirect contact rate without human behavior (resp. shedding rate), b_1 and b_2 describe the associated largest reduced rates caused by human behavior changes, M_1 and M_2 represent the response rates of media and individuals to cholera [41], and $a_i > b_i \geq 0, i = 1, 2$. Here $\hat{\beta}_1(x)$ denotes the indirect transmission rate related to spatial heterogeneity. Similarly, $\hat{\beta}_2(x)$ denotes the shedding rate for *V. cholerae* from infected individuals. We proceed to establish the subsequent biologically inspired hypotheses:

- (H1) Initial conditions $S_0, I_0, B_0 \in C(\bar{\Omega}; \mathbb{R}_+)$ and $(I_0, B_0) \not\equiv 0$ on $\bar{\Omega}$;
- (H2) Functions $\lambda(x), d_i(x) (i = 1, 2, 3), \gamma(x), \delta(x)$ and $\hat{\beta}_i(x) > 0 (i = 1, 2)$ depend on location x , and Hölder continuous.

3. Well-posedness

In this section, various mathematical techniques, including the comparison principle, the strong maximum principle, Sobolev embedding theorem, Gronwall’s inequality, Young’s inequality and interpolation inequality, are employed to establish the existence, uniqueness, nonnegativity, boundedness of solution. Furthermore, the proof of the existence of a global attractor is presented by introducing Kuratowski measure of non-compactness for model (2.1)–(2.3).

For convenience, we always set $u := (S, I, B)^T, d(x) := d_2(x) + \gamma(x) + d_3(x)$ and

$$[\tilde{R}]_M := \max_{x \in \bar{\Omega}} \{ \tilde{R}(x) \} \quad \text{and} \quad [\tilde{R}]_m := \min_{x \in \bar{\Omega}} \{ \tilde{R}(x) \},$$

where $\tilde{R} \in \{ \Lambda, d_i, d, \delta, \hat{\beta}_i (i = 1, 2) \}$. Consider the Banach space $\mathbb{X} := C(\bar{\Omega}, \mathbb{R}^3)$, which represents continuous functions equipped with the supremum norm $\|\phi\|_{\mathbb{X}} := \max(\|\phi_1\|_{\infty}, \|\phi_2\|_{\infty}, \|\phi_3\|_{\infty})$, where $\phi = (\phi_1, \phi_2, \phi_3)^T \in \mathbb{X}$, T represents the transpose of a vector and $\|\psi\|_{\infty} := \sup_{x \in \bar{\Omega}} |\psi(x)|, \forall \psi \in C(\bar{\Omega}, \mathbb{R})$. Let $\mathbb{X}^+ := C(\bar{\Omega}, \mathbb{R}_+^3)$ be the positive cone of \mathbb{X} . For any $\phi^* \in C(\bar{\Omega}, \mathbb{R})$ and $t \geq 0$, denote by $\mathcal{T}_1(t), \mathcal{T}_2(t), \mathcal{T}_3(t) : C(\bar{\Omega}, \mathbb{R}) \rightarrow C(\bar{\Omega}, \mathbb{R})$ the semigroups related to the operators $D_S \Delta - d_1(x), D_I \Delta - d(x), -\delta(x)$, respectively, then

$$\begin{aligned} \mathcal{T}_1(t)\phi^* &= \int_{\Omega} G_1(t, x, y)\phi^*(y)dy, \\ \mathcal{T}_2(t)\phi^* &= \int_{\Omega} G_2(t, x, y)\phi^*(y)dy \end{aligned}$$

and

$$\mathcal{T}_3(t)\phi^* = e^{-\delta(x)t}\phi^*,$$

where G_1 and G_2 are the Green functions corresponding to $D_S \Delta - d_1(x)$ and $D_I \Delta - d(x)$ associated with (2.3), respectively. According to [42, Corollary 7.2.3], we obtain that \mathcal{T}_1 and \mathcal{T}_2 are strongly positive and compact. Moreover, $\mathcal{T}(t) := (\mathcal{T}_1(t), \mathcal{T}_2(t), \mathcal{T}_3(t))^T : \mathbb{X} \rightarrow \mathbb{X}, t \geq 0$ is a strongly continuous semigroup.

Lemma 3.1. *For any $u_0 = (S_0, I_0, B_0)^T \in \mathbb{X}^+$ and a given $\tau_{\max} = \tau_{\max}(u_0) \in [0, \infty]$, then (2.1)–(2.3) exists a unique solution $u(\cdot, t) = u(\cdot, t; u_0)$ on $[0, \tau_{\max})$ for $u(\cdot, 0; u_0) = u_0$. If $\tau_{\max} \in [0, \infty)$, then $\lim_{t \rightarrow \tau_{\max}^-} \sup \|u(\cdot, t)\|_{\mathbb{X}} = \infty$. Moreover, $u(\cdot, t; u_0) \in \mathbb{X}^+$ is a classical solution for $t \in [0, \tau_{\max})$.*

Proof. Obviously, $u(t) =: u(\cdot, t) = (S, I, B)^T$ fulfills

$$u(t) = \mathcal{T}(t)u_0 + \int_0^t \mathcal{T}(t-s)\mathcal{F}(u(s))ds, \quad u_0 = (S_0, I_0, B_0)^T \in \mathbb{X}^+,$$

where $\mathcal{F} : \mathbb{X}^+ \rightarrow \mathbb{X}$ satisfies

$$\mathcal{F}(\phi)(\cdot) := \begin{pmatrix} \mathcal{F}_1(\phi)(\cdot) \\ \mathcal{F}_2(\phi)(\cdot) \\ \mathcal{F}_3(\phi)(\cdot) \end{pmatrix} = \begin{pmatrix} \Lambda(\cdot) - \beta_1(\phi_2, \cdot)\phi_1\phi_3 \\ \beta_1(\phi_2, \cdot)\phi_1\phi_3 \\ \beta_2(\phi_2, \cdot)\phi_2 \end{pmatrix},$$

and $\phi = (\phi_1, \phi_2, \phi_3)^T \in \mathbb{X}^+$. Note that \mathcal{F} is Lipschitz continuous. Then

$$\phi + \ell\mathcal{F}(\phi) = \begin{pmatrix} \phi_1 + \ell[\Lambda(\cdot) - \beta_1(\phi_2, \cdot)\phi_1\phi_3] \\ \phi_2 + \ell\beta_1(\phi_2, \cdot)\phi_1\phi_3 \\ \phi_3 + \ell\beta_2(\phi_2, \cdot)\phi_2 \end{pmatrix} \geq \begin{pmatrix} \phi_1[1 - \ell a_1[\hat{\beta}_1]_M\phi_3] \\ \phi_2 \\ \phi_3 \end{pmatrix}$$

for all $\phi \in \mathbb{X}^+$ and $\ell \geq 0$, which implies that

$$\lim_{\ell \rightarrow 0^+} \frac{1}{\ell} \text{dist}(\phi + \ell\mathcal{F}(\phi), \mathbb{X}^+) = 0$$

for all $\phi \in \mathbb{X}^+$. By [43, Theorem 2 and Corollary 4], we can obtain Lemma 3.1. □

Consider a constant $D > 0$. For any positive continuous functions $\hat{\alpha}(x)$ and $\hat{\beta}(x)$,

$$\begin{cases} \frac{\partial h}{\partial t} = D\Delta h + \hat{\alpha}(x) - \hat{\beta}(x)h, & (x, t) \in \Omega \times (0, \infty), \\ \frac{\partial h}{\partial \nu} = 0, & (x, t) \in \partial\Omega \times (0, \infty), \\ h(x, 0) = h_0(x), & x \in \Omega. \end{cases} \tag{3.1}$$

An application of the results in [44, Lemma 1] yields the following observation.

Lemma 3.2. *System (3.1) exists a unique PSS $h^P(x)$, which is globally asymptotically stable in $C(\bar{\Omega}, \mathbb{R})$. Furthermore, when $\hat{\alpha}(x) \equiv \hat{\alpha}$ and $\hat{\beta}(x) \equiv \hat{\beta}$ are constants, then $h^P(x) = \frac{\hat{\alpha}}{\hat{\beta}}$ is independent of x .*

The global solution of model (2.1)–(2.3) on \mathbb{X}^+ is described below.

Lemma 3.3. *For $u_0 = (S_0, I_0, B_0)^T \in \mathbb{X}^+$, problem (2.1)–(2.3) exists a unique solution*

$$u(\cdot, t; u_0) = (S, I, B)^T \in \mathbb{X}^+$$

on $[0, \infty)$ with $u(\cdot, 0; u_0) = u_0$. Moreover, $u(\cdot, t; u_0)$ is ultimately bounded and uniformly bounded.

Proof. Step 1. The solution $u(\cdot, t; u_0)$ exists globally. Consider the problem

$$\begin{cases} \frac{\partial \tilde{S}}{\partial t} = D_S\Delta \tilde{S} + \Lambda(x) - d_1(x)\tilde{S}, & (x, t) \in \Omega \times (0, \infty), \\ \frac{\partial \tilde{S}}{\partial \nu} = 0, & (x, t) \in \partial\Omega \times (0, \infty), \\ \tilde{S}(x, 0) = S_0(x), & x \in \Omega. \end{cases} \tag{3.2}$$

According to Lemmas 3.1 and 3.2, and the standard comparison principle, one gets

$$0 \leq S \leq \tilde{S} \leq \mathbf{M}_0 := \max \left\{ \frac{[\Lambda]_M}{[d_1]_m}, \|S_0\|_\infty \right\} \tag{3.3}$$

for $(x, t) \in \bar{\Omega} \times [0, \tau_{\max})$. Choosing $K_1 > 0$ large enough satisfying $\|\mathcal{T}_2(t)\|_\infty < K_1 e^{-[d]_m t}$. Let $K_2 = K_1 a_1 [\hat{\beta}_1]_M \mathbf{M}_0$. For $t \in [0, \tau_{\max})$,

$$\begin{aligned} \|I\|_\infty &= \left\| \mathcal{T}_2(t)I_0 + \int_0^t \mathcal{T}_2(t-s)\beta_1(I(\cdot, s), \cdot)S(\cdot, s)B(\cdot, s)ds \right\|_\infty \\ &\leq K_1 e^{-[d]_m t} \|I_0\|_\infty + K_1 a_1 [\hat{\beta}_1]_M \mathbf{M}_0 \int_0^t e^{-[d]_m(t-s)} \|B(\cdot, s)\|_\infty ds \\ &\leq K_1 \|I_0\|_\infty + K_2 \int_0^t e^{-[d]_m(t-s)} \|B(\cdot, s)\|_\infty ds. \end{aligned}$$

By B -equation of (2.1), $\frac{\partial B}{\partial t} \leq a_2 \hat{\beta}_2(\cdot)I - \delta(\cdot)B$, $t \in [0, \tau_{\max})$. Let $\delta_0 = \min\{[d]_m, [\delta]_m\}$, $K_3 = a_2 [\hat{\beta}_2]_M$, the standard comparison principle implies that

$$\begin{aligned} \|B\|_\infty &\leq e^{-[\delta]_m t} \|B_0\|_\infty + a_2 [\hat{\beta}_2]_M \int_0^t e^{-[\delta]_m(t-s)} \|I(\cdot, s)\|_\infty ds \\ &\leq e^{-\delta_0 t} \|B_0\|_\infty + K_3 \int_0^t e^{-\delta_0(t-s)} \|I(\cdot, s)\|_\infty ds \end{aligned}$$

for $t \in [0, \tau_{\max})$. Consequently,

$$\begin{aligned} \|I\|_\infty &\leq K_1 \|I_0\|_\infty + K_2 \int_0^t e^{-[d]_m(t-s)} (e^{-\delta_0 s} \|B_0\|_\infty + K_3 \int_0^s e^{-\delta_0(s-r)} \|I(\cdot, r)\|_\infty dr) ds \\ &\leq K_1 \|I_0\|_\infty + K_2 \|B_0\|_\infty \int_0^t e^{-\delta_0 s} ds + K_2 K_3 e^{-[d]_m t} \int_0^t e^{\delta_0 r} \|I(\cdot, r)\|_\infty \int_r^t e^{([d]_m - \delta_0)s} ds dr \\ &\leq \mathcal{C}_1 + \mathcal{C}_2 e^{-\delta_0 t} \int_0^t e^{\delta_0 r} \|I(\cdot, r)\|_\infty dr, \end{aligned}$$

where $\mathcal{C}_1 = K_1 \|I_0\|_\infty + K_2 \|B_0\|_\infty / \delta_0$, $\mathcal{C}_2 = K_2 K_3 / ([d]_m - \delta_0)$ and $t \in [0, \tau_{\max})$. As Gronwall's inequality, one has

$$\|I\|_\infty \leq \mathcal{C}_1 e^{\mathcal{C}_2 t}, \quad t \in [0, \tau_{\max}). \tag{3.4}$$

Hence,

$$\|B\|_\infty \leq \|B_0\|_\infty + \mathcal{C}_1 e^{\mathcal{C}_2 t} K_3 / \delta_0, \quad t \in [0, \tau_{\max}). \tag{3.5}$$

The above results and Lemma 3.1 imply the global existence of $u(\cdot, t; u_0)$.

Step 2. The boundedness of $\limsup_{t \rightarrow \infty} \|I(\cdot, t)\|_1$ and $\limsup_{t \rightarrow \infty} \|B\|_1$. Combining with (3.3), one can get

$$\|S\|_\infty \leq \mathbf{M}_0, \quad \forall t \geq 0. \tag{3.6}$$

Let $|\Omega|$ be the volume of Ω . We integrate and add the first two formulas of (2.1) to obtain

$$\frac{\partial}{\partial t} \int_\Omega (S + I) dx = \int_\Omega \Lambda(x) dx - \int_\Omega d_1(x) S dx - \int_\Omega d(x) I dx$$

$$\leq [\Lambda]_M |\Omega| - d_4 \int_{\Omega} (S + I) dx,$$

where $d_4 = \min\{[d_1]_m, [d]_m\} > 0$. Let $\|\cdot\|_p$ ($1 \leq p < \infty$) be the L^p -norm, then

$$\limsup_{t \rightarrow \infty} \|I\|_1 \leq \limsup_{t \rightarrow \infty} (\|S(\cdot, t)\|_1 + \|I(\cdot, t)\|_1) \leq \mathbf{M}_1 := [\Lambda]_M |\Omega| / d_4. \tag{3.7}$$

We can choose $t_1 > 0$ satisfying $\|I(\cdot, t)\|_1 \leq \mathbf{M}_1 + 1$ for $t \geq t_1$, then

$$\frac{\partial}{\partial t} \int_{\Omega} B dx \leq a_2 [\hat{\beta}_2]_M \int_{\Omega} I dx - [\delta]_m \int_{\Omega} B dx \leq K_3 (\mathbf{M}_1 + 1) - [\delta]_m \int_{\Omega} B dx, \quad t \geq t_1. \tag{3.8}$$

Hence

$$\limsup_{t \rightarrow \infty} \|B\|_1 \leq K_3 (\mathbf{M}_1 + 1) / [\delta]_m. \tag{3.9}$$

Step 3. For a given $\mathbf{M}_{2^k} > 0$, then

$$\limsup_{t \rightarrow \infty} (\|I\|_{2^k} + \|B(\cdot, t)\|_{2^k}) \leq \mathbf{M}_{2^k}, \tag{3.10}$$

where k represents a nonnegative integer.

Based on the idea of [18, Lemma 2.4], we shall verify (3.10) by mathematical induction. It can be inferred from (3.9) that the case of $k = 0$ holds obviously. Assuming that (3.10) holds for $k - 1 \geq 0$, we can choose $\mathbf{M}_{2^{k-1}} > 0$ satisfying

$$\limsup_{t \rightarrow \infty} (\|I\|_{2^{k-1}} + \|B\|_{2^{k-1}}) \leq \mathbf{M}_{2^{k-1}}. \tag{3.11}$$

We multiply the I -equation of (2.1) by I^{2^k-1} and integrate over Ω to yield

$$\frac{1}{2^k} \frac{\partial}{\partial t} \int_{\Omega} I^{2^k} dx = D_I \int_{\Omega} I^{2^k-1} \Delta I dx + \int_{\Omega} \beta_1(I, x) S B I^{2^k-1} dx - \int_{\Omega} d(x) I^{2^k} dx. \tag{3.12}$$

Note that

$$\begin{aligned} D_I \int_{\Omega} I^{2^k-1} \Delta I dx &\leq -D_I \int_{\Omega} \nabla I \cdot \nabla I^{2^k-1} dx = -(2^k - 1) D_I \int_{\Omega} (\nabla I \cdot \nabla I) I^{2^k-2} dx \\ &= -\frac{2^k - 1}{2^{2^k-2}} D_I \int_{\Omega} |\nabla I^{2^k-1}|^2 dx. \end{aligned}$$

With (3.6), we know

$$\int_{\Omega} \beta_1(I, x) S B I^{2^k-1} dx \leq a_1 [\hat{\beta}_1]_M (\mathbf{M}_0 + 1) \int_{\Omega} B I^{2^k-1} dx.$$

Now, we use the Young's inequality $\tilde{a}\tilde{b} \leq \epsilon\tilde{a}^p + C_\epsilon\tilde{b}^q$, where $\tilde{a}, \tilde{b}, \epsilon, q > 0, p > 1, C_\epsilon = (\epsilon p)^{-q/p} q^{-1}$ and $p^{-1} + q^{-1} = 1$.

We can choose $\epsilon_1 = \frac{[\delta]_m}{4a_1[\hat{\beta}_1]_M(\mathbf{M}_0+1)}$, $p = 2^k$ and $q = 2^k/(2^k - 1)$ satisfying

$$\int_{\Omega} B I^{2^k-1} dx \leq \frac{[\delta]_m}{4a_1[\hat{\beta}_1]_M(\mathbf{M}_0+1)} \int_{\Omega} B^{2^k} dx + C_{\epsilon_1} \int_{\Omega} I^{2^k} dx.$$

Let $E_k = \frac{2^k-1}{2^{2k-2}}D_I$, $C_k = a_1[\hat{\beta}_1]_M(\mathbf{M}_0 + 1)C_{\epsilon_1}$, then

$$\frac{1}{2^k} \frac{\partial}{\partial t} \int_{\Omega} I^{2^k} dx \leq -E_k \int_{\Omega} |\nabla I^{2^{k-1}}|^2 dx + \frac{[\delta]_m}{4} \int_{\Omega} B^{2^k} dx + C_k \int_{\Omega} I^{2^k} dx. \tag{3.13}$$

Then we conduct the multiplication of the B -equation in (2.1) by B^{2^k-1} and perform an integration over Ω to get

$$\begin{aligned} \frac{1}{2^k} \frac{\partial}{\partial t} \int_{\Omega} B^{2^k} dx &= \int_{\Omega} \beta_2(I, x)IB^{2^k-1}dx - \int_{\Omega} \delta(x)B^{2^k} dx \\ &\leq K_3 \int_{\Omega} IB^{2^k-1}dx - [\delta]_m \int_{\Omega} B^{2^k} dx. \end{aligned}$$

Again, applying Young’s inequality with $\epsilon_2 = \frac{[\delta]_m}{4K_3}$, $p = 2^k/(2^k - 1)$ and $q = 2^k$, we get

$$\int_{\Omega} IB^{2^k-1}dx \leq \frac{[\delta]_m}{4K_3} \int_{\Omega} B^{2^k} dx + C_{\epsilon_2} \int_{\Omega} I^{2^k} dx,$$

then

$$\frac{1}{2^k} \frac{\partial}{\partial t} \int_{\Omega} B^{2^k} dx \leq K_3C_{\epsilon_2} \int_{\Omega} I^{2^k} dx - \frac{3[\delta]_m}{4} \int_{\Omega} B^{2^k} dx. \tag{3.14}$$

This, together with (3.13), implies that

$$\frac{1}{2^k} \frac{\partial}{\partial t} \int_{\Omega} (I^{2^k} + B^{2^k})dx \leq -E_k \int_{\Omega} |\nabla I^{2^{k-1}}|^2 dx - \frac{[\delta]_m}{2} \int_{\Omega} B^{2^k} dx + \tilde{C}_k \int_{\Omega} I^{2^k} dx, \tag{3.15}$$

where $\tilde{C}_k = C_k + K_3C_{\epsilon_2}$.

Next, we apply the interpolation inequality, i.e., $\forall \epsilon_* > 0$, we can choose $C_{\epsilon_*} > 0$ satisfying

$$\|\zeta\|_2^2 \leq \epsilon_*\|\nabla\zeta\|_2^2 + C_{\epsilon_*}\|\zeta\|_1^2, \quad \forall \zeta \in W^{1,2}(\Omega).$$

Let $\zeta = I^{2^{k-1}}$ and $\epsilon_* = E_k/(2\tilde{C}_k)$, we have

$$-E_k \int_{\Omega} |\nabla I^{2^{k-1}}|^2 dx \leq -2\tilde{C}_k \int_{\Omega} I^{2^k} dx + 2\tilde{C}_kC_{\epsilon_*} \left(\int_{\Omega} I^{2^{k-1}} dx \right)^2.$$

Take $\delta_* = \min\{\tilde{C}_k, [\delta]_m/2\}$, then (3.15) fulfills

$$\begin{aligned} \frac{1}{2^k} \frac{\partial}{\partial t} \int_{\Omega} (I^{2^k} + B^{2^k})dx &\leq -\tilde{C}_k \int_{\Omega} I^{2^k} dx + 2\tilde{C}_kC_{\epsilon_*} \left(\int_{\Omega} I^{2^{k-1}} dx \right)^2 - \frac{[\delta]_m}{2} \int_{\Omega} B^{2^k} dx \\ &\leq -\delta_* \int_{\Omega} (I^{2^k} + B^{2^k})dx + 2\tilde{C}_kC_{\epsilon_*} \left(\int_{\Omega} I^{2^{k-1}} dx \right)^2. \end{aligned} \tag{3.16}$$

In view of (3.11), we obtain

$$\limsup_{t \rightarrow \infty} \int_{\Omega} I^{2^{k-1}} dx \leq \mathbf{M}_{2^{k-1}}^{2^{k-1}},$$

then

$$\limsup_{t \rightarrow \infty} (\|I\|_{2^k} + \|B\|_{2^k}) \leq \sqrt[2^k]{\frac{2\tilde{C}_k C_{\epsilon_*}}{\delta_*} \mathbf{M}_{2^{k-1}}} =: \mathbf{M}_{2^k}.$$

Therefore, (3.10) holds for any nonnegative integer k .

Step 4. The ultimately boundedness of $u(\cdot, t)$ in \mathbb{X}^+ . Inspired by [18, Claim 4 of Lemma 2.4], we denote by $\mathcal{T}_2(t)$ the analytic semigroup with respect to $A_2 := D_I \Delta - d(\cdot)$ in $Y = L^p(\Omega)$, where $D(A_2) = \{u \in W^{2,p} \text{ and } \frac{\partial u}{\partial \nu} = 0 \text{ in } \partial\Omega\}$. Denoted by Y_a , $0 \leq a < 1$, the fractional power space equipped with the graph norm. We can find $p > n/2$ and $a > n/(2p)$ satisfying $Y_a \subset C(\bar{\Omega})$. On the other hand, the continuous embedding $L^s(\Omega) \subset L^r(\Omega)$ holds for $s \geq r \geq 1$.

For any $n \geq 1$, we can find p and k satisfying $2^k \geq p > n/2$. By (3.10), one can get

$$\limsup_{t \rightarrow \infty} (\|I\|_p + \|B\|_p) \leq \mathbf{M}_p, \tag{3.17}$$

where \mathbf{M}_p is a positive constant. With the help of [18, Claim 4 of Lemma 2.4], we can choose $\mathbf{M}_a > 0$ satisfying $\|A_2^a \mathcal{T}_2(t)\|_\infty \leq \mathbf{M}_a/t^a, \forall t > 0$. According to (3.6) and (3.17), there is a $t_2 > 1$ satisfying

$$\|S\|_\infty \leq \mathbf{M}_0, \|I\|_p \leq \mathbf{M}_p + 1 \text{ and } \|B\|_p \leq \mathbf{M}_p + 1, \forall t > t_2 - 1.$$

Then

$$\begin{aligned} \|A_2^a I\|_p &\leq \|A_2^a \mathcal{T}_2(1)I(\cdot, t-1)\|_p + \int_{t-1}^t \|A_2^a \mathcal{T}_2(t-s)\beta_1(I(\cdot, s), \cdot)S(\cdot, s)B(\cdot, s)\|_p ds \\ &\leq \mathbf{M}_a \|I(\cdot, t-1)\|_p + a_1[\hat{\beta}_1]_M \mathbf{M}_0 (\mathbf{M}_p + 1) \int_{t-1}^t \frac{\mathbf{M}_a}{(t-s)^a} ds \\ &\leq \mathbf{M}_a (\mathbf{M}_p + 1) + \frac{a_1[\hat{\beta}_1]_M \mathbf{M}_0 (\mathbf{M}_p + 1) \mathbf{M}_a}{1-a} \end{aligned}$$

for any $t > t_2 - 1$. By $Y_a \subset C(\bar{\Omega})$, we obtain

$$\limsup_{t \rightarrow \infty} \|I\|_\infty \leq \bar{\mathbf{M}}, \tag{3.18}$$

where $\bar{\mathbf{M}} > 0$ is a constant. Then we are able to select $t_3 > 0$ satisfying $\|I(\cdot, t)\|_\infty \leq \bar{\mathbf{M}} + 1$ for $t \geq t_3$. According to the B -equation of (2.1), one obtains

$$\limsup_{t \rightarrow \infty} \|B\|_\infty \leq \frac{K_3(\bar{\mathbf{M}} + 1)}{[\delta]_m}.$$

Step 5. The uniformly boundedness of $u(\cdot, t; u_0)$. For every given initial condition $u_0 \in \mathbb{X}^+$, we can find a constant $\mathbf{M}_\infty > 0$ satisfying

$$\|S\|_\infty + \|I\|_\infty + \|B\|_\infty \leq \mathbf{M}_\infty, \forall t \in [0, \infty). \tag{3.19}$$

Lemma 3.3 is proved. □

According to [18], the subsequent result substantiates the existence of the global attractor.

Lemma 3.4. *Model (2.1)–(2.3) exists a global attractor in \mathbb{X}^+ .*

Proof. Denote by $\Upsilon(t) : \mathbb{X}^+ \rightarrow \mathbb{X}^+ (t \geq 0)$ the semiflow associated with (2.1)–(2.3). It follows from [42, Theorem 3.1 (d) in Chapter 7] that $\Upsilon(t) : \mathbb{X}^+ \rightarrow \mathbb{X}^+ (t \geq 0)$ fulfills

$$\Upsilon(t)u_0 = (S(\cdot, t; u_0), I(\cdot, t; u_0), B(\cdot, t; u_0))^T.$$

Note that the non-compactness of $\Upsilon(t)$ is attributed to the absence of a dispersal term in B -equation of (2.1). However, we will prove that $\Upsilon(t)$ is κ -contraction. It follows from [45, Lemma 2.3.4] that Kuratowski measure of non-compactness represents

$$\kappa(\mathbb{B}) := \inf\{r : \mathbb{B} \text{ has a finite cover of diameter } < r\} \tag{3.20}$$

for any bounded $\mathbb{B} \subset \mathbb{X}^+$. It can be readily observed that \mathbb{B} is precompact if and only if $\kappa(\mathbb{B}) = 0$. According to the B -equations of (2.1), one can define

$$G(I, B) = \beta_2(I, \cdot)I - \delta(\cdot)B.$$

Hence

$$\frac{\partial G(I, B)}{\partial B} = -\delta(\cdot) \leq -[\delta]_m.$$

According to [18, Lemma 2.6], one can decompose $\Upsilon(t) = \Upsilon_1(t) + \Upsilon_2(t)$, where

$$\Upsilon_1(t)u_0 = \left(S(\cdot, t; u_0), I(\cdot, t; u_0), \int_0^t e^{-\delta(\cdot)(t-s)} \beta_2(I(\cdot, s; u_0), \cdot) I(\cdot, s; u_0) ds \right)^T$$

and

$$\Upsilon_2(t)u_0 = \left(0, 0, e^{-\delta(\cdot)t} B_0 \right)^T, \quad \forall t \geq 0.$$

By similar arguments as [18, Lemma 2.5], we can obtain that

$$\mathcal{S}_1 = \left\{ \int_0^t e^{-\delta(\cdot)(t-s)} \beta_2(I(\cdot, s; u_0), \cdot) I(\cdot, s; u_0) ds \right\}$$

is precompact for all $u_0 \in \mathbb{B}$ and $t > 0$. Hence $\kappa(\Upsilon_1(t)\mathbb{B}) = 0, \forall t > 0$. On the other hand,

$$\|\Upsilon_2(t)\|_{\text{op}} = \sup_{u_0 \in \mathbb{X}, \|u_0\|_{\mathbb{X}} \neq 0} \frac{\|\Upsilon_2(t)u_0\|_{\mathbb{X}}}{\|u_0\|_{\mathbb{X}}} \leq \sup_{u_0 \in \mathbb{X}, \|u_0\|_{\mathbb{X}} \neq 0} \frac{\|u_0\|_{\mathbb{X}}}{\|u_0\|_{\mathbb{X}}} \cdot e^{-[\delta]_m t} = e^{-[\delta]_m t},$$

where $\|\cdot\|_{\text{op}}$ represents the operator norm. Hence,

$$\kappa(\Upsilon(t)\mathbb{B}) \leq \kappa(\Upsilon_1(t)\mathbb{B}) + \kappa(\Upsilon_2(t)\mathbb{B}) \leq 0 + \|\Upsilon_2(t)\|_{\text{op}} \kappa(\mathbb{B}) \leq e^{-[\delta]_m t} \kappa(\mathbb{B}), \quad t > 0.$$

Hence $\Upsilon(t)$ is κ -contraction. Moreover, it is deduced from [45, Lemma 2.3.4] that $\Upsilon(t)$ is asymptotically smooth. According to Lemma 3.3, $\Upsilon(t)$ is point dissipative. In accordance with [45, Theorem 2.4.6], Lemma 3.4 is proved. □

4. Threshold dynamics

In this section, we establish \mathfrak{R}_0 by analyzing the correlative eigenvalue problem of system (2.1)–(2.3) at the IFSS, where \mathfrak{R}_0 denotes the anticipated count of secondary infections resulting from a single index infection within an otherwise susceptible population [17]. Moreover, we also study how \mathfrak{R}_0 responds to changes in several model parameters. Then the global dynamics of system (2.1)–(2.3) is investigated through the application of \mathfrak{R}_0 .

4.1. Basic reproduction number

Let $I = B = 0$. Then model (2.1)–(2.3) has a unique IFSS $E_0 = (S^P(x), 0, 0)$ by Lemma 3.2. Linearizing model (2.1)–(2.3) at E_0 and denoting

$$\mathcal{B} = \begin{pmatrix} D_I \Delta - d(x) & a_1 \hat{\beta}_1(x) S^P(x) \\ a_2 \hat{\beta}_2(x) & -\delta(x) \end{pmatrix}, \tag{4.1}$$

we have

$$\begin{cases} \frac{\partial \bar{u}}{\partial t} = \mathcal{B} \bar{u}, & (x, t) \in \Omega \times (0, \infty), \\ \frac{\partial \bar{I}}{\partial t} = 0, & (x, t) \in \partial\Omega \times (0, \infty), \\ \frac{\partial \bar{\vartheta}}{\partial t} = 0, & (x, t) \in \partial\Omega \times (0, \infty), \\ \bar{u}(x, 0) = \bar{u}_0(x) & x \in \Omega, \end{cases} \tag{4.2}$$

where $\bar{u} = (I, B)^T$ and $\bar{u}_0 = (I_0, B_0)^T$. Then we introduce linear operators

$$B = \begin{pmatrix} D_I \Delta - d(x) & 0 \\ a_2 \hat{\beta}_2(x) & -\delta(x) \end{pmatrix}, \quad F = \begin{pmatrix} 0 & a_1 \hat{\beta}_1(x) S^P(x) \\ 0 & 0 \end{pmatrix}.$$

Denote by $\tilde{Y}(t), \tilde{Y}(t) : C(\bar{\Omega}, \mathbb{R}^2) \rightarrow C(\bar{\Omega}, \mathbb{R}^2)$ the C_0 -semigroups corresponding to \mathcal{B} and B , respectively, where $\mathcal{B} = B + F$. We assume that $\phi \in C(\bar{\Omega}, \mathbb{R}^2)$ represents the distribution of initial condition. Hence $\tilde{Y}(t)\phi$ signifies the distribution of infectious individuals as time evolves. Consequently, $F\tilde{Y}(t)\phi$ represents the distribution of fresh infections individuals at t . According to [34, 47], we introduce the next generation operator

$$\mathcal{L}\phi = \int_0^\infty F\tilde{Y}(t)\phi dt = F \int_0^\infty \tilde{Y}(t)\phi dt, \quad \phi \in C(\bar{\Omega}, \mathbb{R}^2) \tag{4.3}$$

and establish \mathfrak{R}_0 to represent the spectral radius of \mathcal{L} , namely,

$$\mathfrak{R}_0 := r(\mathcal{L}).$$

According to [47, Theorem 3.5] and [34, Theorem 3.1], we have the following result.

Lemma 4.1. *Denoted by $s(\mathcal{B})$ the spectral bound of \mathcal{B} . Then $\mathfrak{R}_0 - 1$ and $s(\mathcal{B})$ have the same sign.*

Theorem 4.2. (i) *Let $\tilde{\lambda}_1$ be the principal eigenvalue of*

$$\begin{cases} -D_I \Delta \psi + d(x)\psi = \tilde{\lambda} \frac{a_1 a_2 \hat{\beta}_1(x) \hat{\beta}_2(x) S^P(x)}{\delta(x)} \psi, & x \in \Omega, \\ \frac{\partial \psi}{\partial \nu} = 0, & x \in \partial\Omega, \\ \psi \in C^2(\Omega, \mathbb{R}^n) \cap C^1(\bar{\Omega}, \mathbb{R}^n), \end{cases} \tag{4.4}$$

then

$$\mathfrak{R}_0 = \frac{1}{\tilde{\lambda}_1} = \sup_{\psi \in H^1(\Omega), \psi \neq 0} \frac{\int_\Omega \frac{a_1 a_2 \hat{\beta}_1(x) \hat{\beta}_2(x) S^P(x)}{\delta(x)} \psi^2 dx}{\int_\Omega [D_I |\nabla \psi|^2 + d(x)\psi^2] dx}. \tag{4.5}$$

Moreover, \mathfrak{R}_0 is decreasing in D_I ; \mathfrak{R}_0 is increasing with respect to a_1 or a_2 .

(ii) For any $D_S > 0$,

$$\lim_{D_I \rightarrow 0} \mathfrak{R}_0 = \max_{x \in \Omega} \left\{ \frac{a_1 a_2 \hat{\beta}_1(x) \hat{\beta}_2(x) S^P(x)}{\delta(x) d(x)} \right\} \tag{4.6}$$

and

$$\lim_{D_I \rightarrow \infty} \mathfrak{R}_0 = \frac{\int_{\Omega} \left(\frac{a_1 a_2 \hat{\beta}_1(x) \hat{\beta}_2(x) S^P(x)}{\delta(x)} \right) dx}{\int_{\Omega} d(x) dx}. \tag{4.7}$$

(iii) If $\int_{\Omega} \left(\frac{a_1 a_2 \hat{\beta}_1(x) \hat{\beta}_2(x) S^P(x)}{\delta(x)} \right) dx > \int_{\Omega} d(x) dx$, then $\mathfrak{R}_0 > 1$, $\forall D_I > 0$.

(iv) If $\int_{\Omega} \left(\frac{a_1 a_2 \hat{\beta}_1(x) \hat{\beta}_2(x) S^P(x)}{\delta(x)} \right) dx < \int_{\Omega} d(x) dx$ and $\frac{a_1 a_2 \hat{\beta}_1(x) \hat{\beta}_2(x) S^P(x)}{\delta(x) d(x)} > 1$ for some $x \in \Omega$, then there exists a $\hat{D}_I > 0$ satisfying $\mathfrak{R}_0 < 1$ if $D_I > \hat{D}_I$, while $\mathfrak{R}_0 > 1$ if $D_I < \hat{D}_I$.

Proof. (i) According to [48, Remark 1.6], the eigenvalue $\tilde{\lambda}_1 > 0$ is unique for (4.4) with a positive eigenfunction. Using a similar approach in [34, Theorem 3.3], one can gain

$$\mathfrak{R}_0 = r \left(-[D_I \Delta - d(x)]^{-1} \frac{a_1 a_2 \hat{\beta}_1(x) \hat{\beta}_2(x) S^P(x)}{\delta(x)} \right).$$

Hence, for $\psi \in C^2(\Omega, \mathbb{R}^n) \cap C^1(\bar{\Omega}, \mathbb{R}^n)$, \mathfrak{R}_0 fulfills

$$\left(-[D_I \Delta - d(x)]^{-1} \frac{a_1 a_2 \hat{\beta}_1(x) \hat{\beta}_2(x) S^P(x)}{\delta(x)} \right) \psi = \mathfrak{R}_0 \psi,$$

i.e.,

$$-D_I \Delta \psi + d(x) \psi = \frac{a_1 a_2 \hat{\beta}_1(x) \hat{\beta}_2(x) S^P(x)}{\delta(x)} \frac{1}{\mathfrak{R}_0} \psi. \tag{4.8}$$

By a similar argument as [49], $\mathfrak{R}_0 = \frac{1}{\tilde{\lambda}_1}$ can be written as (4.5). This proves (i). According to (4.5) and [49, Theorem 2], one can gain (ii)-(iv). □

The variational characterization of \mathfrak{R}_0 as outlined in Theorem 4.2 (i) establishes it as a monotonically decreasing function with respect to dispersal coefficient (D_I) of infected individuals and depends on dispersal coefficient (D_S) of susceptible individuals through the influence of D_S on S^P . Furthermore, augmenting the rates of indirect contact or shedding is anticipated to increase the infection risk. Nevertheless, \mathfrak{R}_0 does not exhibit dependence on the parameters b_i or M_i ($i = 1, 2$) associated with human behavior change. Theorem 4.2 (ii) asserts that \mathfrak{R}_0 converges to the maximum local reproduction number as D_I approaches infinitesimal value, and it tends to an average value as D_I becomes arbitrarily large. Theorem 4.2 (iii) and (iv) suggest that it is possible to regulate R_0 in terms of D_I in some cases.

To ascertain adequate conditions for the either extinction or persistence of cholera, ensuing the following theorem examines the interplay between \mathfrak{R}_0 and the eigenvalue problems linked with model (2.1)–(2.3).

Theorem 4.3. (i) Denoted by η_1 the principal eigenvalue of

$$\begin{cases} D_I \Delta \varphi - d(x)\varphi + \frac{a_1 a_2 \hat{\beta}_1(x) \hat{\beta}_2(x) S^P(x)}{\delta(x)} \varphi = \eta \varphi, & x \in \Omega, \\ \frac{\partial \varphi}{\partial \nu} = 0, & x \in \partial \Omega, \\ \varphi \in C^2(\Omega, \mathbb{R}^n) \cap C^1(\bar{\Omega}, \mathbb{R}^n), \end{cases} \tag{4.9}$$

then $\Re_0 - 1$, $s(\mathcal{B})$ and η_1 have the same sign;

(ii) If $\Re_0 \geq 1$ or $\delta(x) \equiv \delta$, then $s(\mathcal{B})$ is the principal eigenvalue of

$$\begin{cases} \lambda \begin{pmatrix} \psi_2 \\ \psi_3 \end{pmatrix} = \mathcal{B} \begin{pmatrix} \psi_2 \\ \psi_3 \end{pmatrix}, & x \in \Omega, \\ \frac{\partial \psi_2}{\partial \nu} = 0, & x \in \partial \Omega, \\ \psi_2 \in C^2(\Omega, \mathbb{R}) \cap C^1(\bar{\Omega}, \mathbb{R}), \psi_3 \in C(\bar{\Omega}, \mathbb{R}). \end{cases} \tag{4.10}$$

Proof. (i) By [48, Remark 1.6], let η_1 be the principal eigenvalue of (4.9) with a positive eigenfunction φ^* , then

$$D_I \Delta \varphi^* - d(x)\varphi^* + \frac{a_1 a_2 \hat{\beta}_1(x) \hat{\beta}_2(x) S^P(x)}{\delta(x)} \varphi^* = \eta_1 \varphi^*, \text{ for } x \in \Omega \tag{4.11}$$

with homogeneous Neumann boundary condition. By multiplying (4.11) by ψ and (4.8) by φ^* , respectively, then subtracting them and integrating the result, one can obtain

$$\left(1 - \frac{1}{\Re_0}\right) a_1 a_2 \int_{\Omega} \frac{\hat{\beta}_1(x) \hat{\beta}_2(x) S^P(x)}{\delta(x)} \psi \varphi^* dx = \eta_1 \int_{\Omega} \psi \varphi^* dx.$$

Obviously, $1 - \frac{1}{\Re_0}$ have the same sign as η_1 .

(ii) Case. 1: $\Re_0 \geq 1$. Problem (4.2) implies

$$\begin{cases} I(\cdot, t; \phi) = \mathcal{T}_2(t)\phi_2 + \int_0^t \mathcal{T}_2(t-s) a_1 \hat{\beta}_1(\cdot) S^P(\cdot) B(\cdot, s; \phi) ds, \\ B(\cdot, t; \phi) = \mathcal{T}_3(t)\phi_3 + \int_0^t \mathcal{T}_3(t-s) a_2 \hat{\beta}_2(\cdot) I(\cdot, s; \phi) ds, \end{cases}$$

with $\phi = (\phi_2, \phi_3)^T \in C(\bar{\Omega}, \mathbb{R}^2)$. Obviously, $\bar{\Upsilon}(t) = \bar{\Upsilon}_2(t) + \bar{\Upsilon}_3(t)$, where

$$\bar{\Upsilon}_2(t)\phi = (0, \mathcal{T}_3(t)\phi_3)^T, \phi = (\phi_2, \phi_3) \in C(\bar{\Omega}, \mathbb{R}^2), \tag{4.12}$$

and

$$\bar{\Upsilon}_3(t)\phi = \left(I(\cdot, t; \phi), \int_0^t \mathcal{T}_3(t-s) a_2 \hat{\beta}_2(\cdot) I(\cdot, s; \phi) ds \right)^T, \phi = (\phi_2, \phi_3) \in C(\bar{\Omega}, \mathbb{R}^2).$$

Based on [18, Lemma 2.5], it can be deduced that $\bar{\Upsilon}_3(t)$ is compact. However, for every bounded set \mathbb{B} in $C(\bar{\Omega})$, Lemmas 3.4 and (4.12) imply that

$$\kappa(\bar{\Upsilon}(t)\mathbb{B}) \leq e^{-[\delta]_m t} \kappa(\mathbb{B}), \quad t > 0. \tag{4.13}$$

Let

$$\alpha(\tilde{L}) := \inf_{\mathbb{B} \subset \mathbb{X}^+ \text{ is bounded}} \{ \epsilon > 0 : \kappa(\tilde{L}\mathbb{B}) \leq \epsilon \kappa(\mathbb{B}) \}$$

be the measure of non-compactness of operator on \mathbb{X}^+ . Denoted by $\omega_{ess}(\tilde{\Upsilon}) := \lim_{t \rightarrow \infty} \frac{\ln \alpha(\tilde{\Upsilon}(t))}{t}$ the essential growth bound of $\tilde{\Upsilon}$. According to (4.13), one can obtain that $\omega_{ess}(\tilde{\Upsilon}) \leq -[\delta]_m$ and

$$r_e(\tilde{\Upsilon}(t)) \leq e^{-[\delta]_m t} < 1, \quad t > 0,$$

where $r_e(\tilde{\Upsilon}(t))$ is the essential spectral radius of $\tilde{\Upsilon}(t)$. The exponential growth bound of $\tilde{\Upsilon}$ is defined as

$$\omega(\tilde{\Upsilon}) := \inf \left\{ \tilde{\omega} \in \mathbb{R} : \text{there is a } \hat{M} \geq 1 \text{ such that } \|\tilde{\Upsilon}(t)\|_{op} \leq \hat{M}e^{\tilde{\omega}t}, \forall t \geq 0 \right\},$$

where $\|\cdot\|_{op}$ is defined in the proof of Lemma 3.4. Additionally,

$$\omega(\tilde{\Upsilon}) = \max\{s(\mathcal{B}), \omega_{ess}(\tilde{\Upsilon})\}.$$

With the help of (i) of Theorem 4.3, we have $s(\mathcal{B}) \geq 0$ for $\mathfrak{R}_0 \geq 1$. Hence, $r(\tilde{\Upsilon}(t)) = e^{s(\mathcal{B})t} \geq 1, \forall t > 0$, which implies that $r_e(\tilde{\Upsilon}(t)) < r(\tilde{\Upsilon}(t))$. By generalized Krein-Rutman theorem [50, lemma 2.2], one can obtain that $s(\mathcal{B})$ is the principal eigenvalue of (4.10).

Case. 2: $\delta(x) \equiv \delta$. Define $\mathcal{L}_\lambda = D_I \Delta - d(x) + a_1 \hat{\beta}_1(x) S^P(x) a_2 \hat{\beta}_2(x) / (\lambda + \delta), \lambda > -\delta$ with Neumann boundary condition, which is usually called the one-parameter family of linear operators. Obviously, $s(\mathcal{L}_\lambda)$ decreases as λ increases. Inspired by [49],

$$\begin{cases} D_I \Delta \varphi - d(x)\varphi = \eta \varphi, & x \in \Omega, \\ \frac{\partial \varphi}{\partial \nu} = 0, & x \in \partial \Omega \end{cases}$$

exists a principle eigenvalue

$$\eta_* = \sup \left\{ \int_{\Omega} [-D_I |\nabla \varphi|^2 - d(x)\varphi^2] dx \mid \int_{\Omega} \varphi^2 dx = 1, \varphi \in H^1(\Omega) \right\}$$

with eigenfunction $\varphi_0 \gg 0$.

Denote $\mathcal{C} := \min_{x \in \bar{\Omega}} \{a_1 a_2 \hat{\beta}_1(x) S^P(x) \hat{\beta}_2(x)\}$. Let $\hat{\lambda} = \frac{1}{2}[(\eta_* - \delta) + \sqrt{(\eta_* + \delta)^2 + 4\mathcal{C}}]$ be the positive solution of

$$\lambda^2 + (\delta - \eta_*)\lambda - (\delta\eta_* + \mathcal{C}) = 0.$$

Hence, $\hat{\lambda} > -\delta$. For any $\varphi^0 > 0$, we have

$$\begin{aligned} \mathcal{L}_{\hat{\lambda}} \varphi^0 &= D_I \Delta \varphi^0 + \frac{a_1 \hat{\beta}_1(\cdot) S^P(\cdot) a_2 \hat{\beta}_2(\cdot)}{(\lambda + \delta)} \varphi^0 - d(\cdot) \varphi^0 \\ &\geq (\eta_* + \frac{\mathcal{C}}{\hat{\lambda} + \delta}) \varphi^0 = \hat{\lambda} \varphi^0. \end{aligned}$$

It follows from [37, Lemma 2.6] and [34, Theorem 2.3] that (ii) holds. □

4.2. Dynamics for $\mathfrak{R}_0 < 1$

This subsection will study the global stability of the IFSS $E_0 = (S^P(x), 0, 0)$ when $\mathfrak{R}_0 < 1$, which implies that the disease dies out. According to [34, Theorem 3.1], one can obtain the local asymptotic stability of E_0 . To obtain that E_0 is globally asymptotically stable, we will confirm Theorem 4.4.

Theorem 4.4. *For $\mathfrak{R}_0 < 1, E_0$ is globally asymptotically attractive.*

Proof. According to Lemma 3.3, fix $\epsilon_0 > 0$, there is $t_7 > 0$ satisfying

$$0 \leq S \leq S^P(x) + \epsilon_0, \quad \forall \bar{\Omega} \times [t_7, \infty).$$

Set

$$\mathcal{B}_{\epsilon_0} = \begin{pmatrix} D_I \Delta - d(x) & a_1 \hat{\beta}_1(x)(S^P(x) + \epsilon_0) \\ a_2 \hat{\beta}_2(x) & -\delta(x) \end{pmatrix}.$$

Let $(\hat{I}, \hat{B})(x, t)$ satisfying

$$\begin{cases} \begin{pmatrix} \frac{\partial \hat{I}}{\partial t} \\ \frac{\partial \hat{B}}{\partial t} \end{pmatrix} = \mathcal{B}_{\epsilon_0} \begin{pmatrix} \hat{I} \\ \hat{B} \end{pmatrix}, & (x, t) \in \Omega \times (t_7, \infty), \\ \frac{\partial \hat{I}}{\partial \vartheta} = 0, & (x, t) \in \partial\Omega \times (t_7, \infty). \end{cases} \quad (4.14)$$

The comparison principle implies

$$(I, B) \leq (\hat{I}, \hat{B}) \text{ on } \bar{\Omega} \times (t_7, \infty).$$

Denoted by $\tilde{Y}_{\epsilon_0}(t)$ the C_0 semigroup corresponding to \mathcal{B}_{ϵ_0} . By using a similar argument as in Lemma 3.4, one can get $\omega_{ess}(\tilde{Y}_{\epsilon_0}) \leq -[\delta]_m$. Let $\omega_{\epsilon_0} := \omega(\tilde{Y}_{\epsilon_0})$. Note that $\omega_{\epsilon_0} = \max\{s(\mathcal{B}_{\epsilon_0}), \omega_{ess}(\tilde{Y}_{\epsilon_0})\}$. Consequently, ω_{ϵ_0} and $s(\mathcal{B}_{\epsilon_0})$ possess the same sign. Moreover, Theorem 4.3 (i) implies that $s(\mathcal{B}_{\epsilon_0})$ and η_{ϵ_0} possess the same sign, where η_{ϵ_0} represents the principal eigenvalue of

$$\begin{cases} D_I \Delta \varphi - d(x)\varphi + \frac{a_1 a_2 \hat{\beta}_1(x) \hat{\beta}_2(x)(S^P(x) + \epsilon_0)}{\delta(x)} \varphi = \eta \varphi, & x \in \Omega, \\ \frac{\partial \varphi}{\partial \vartheta} = 0, & x \in \partial\Omega. \end{cases}$$

By Theorem 4.3 (i) and $\mathfrak{R}_0 < 1$, one can get $\eta_1 < 0$. By continuity of η_{ϵ_0} in ϵ_0 , there is $\epsilon_0 > 0$ satisfying $\eta_{\epsilon_0} < 0$. Thus $\omega_{\epsilon_0} < 0$. Further there is $\tilde{M} > 0$ satisfying

$$\|\tilde{Y}_{\epsilon_0}(t)\|_{op} \leq \tilde{M} e^{\omega_{\epsilon_0} t}, \quad \forall t \geq 0.$$

Then

$$\lim_{t \rightarrow \infty} (I, B) = (0, 0), \quad \forall x \in \bar{\Omega}.$$

This result together with Lemma 3.2 implies that E_0 is globally asymptotically attractive. □

4.3. Uniform persistence for $\mathfrak{R}_0 > 1$

This subsection aims to explore the persistence of infection and the existence of PSS when $\mathfrak{R}_0 > 1$, which indicates the uniform persistence of cholera in the presence of infected human hosts or free-living pathogens in the reservoir. First, we present three lemmas that will be used repeatedly in what follows.

Lemma 4.5. For $u_0 \in \mathbb{X}^+$ and $(x, t) \in \bar{\Omega} \times (0, \infty)$, we have

$$S(x, t; u_0) > 0. \quad (4.15)$$

Furthermore, there exists $\sigma_1 > 0$ satisfying

$$\liminf_{t \rightarrow \infty} S(x, t; u_0) \geq \sigma_1, \quad \text{uniformly for } x \in \bar{\Omega}. \quad (4.16)$$

Proof. For $(x, t) \in \bar{\Omega} \times [0, \infty)$, Lemma 3.3 implies $S(x, t) \geq 0$. By contradiction, there exists $(x_4, t_4) \in \bar{\Omega} \times (0, \infty)$ satisfying $S(x_4, t_4) = 0$ and $S(x, t) > 0$ for $t < t_4$, then S is minimum at (x_4, t_4) . If $x_4 \in \partial\Omega$, the Hopf boundary lemma implies $\frac{\partial S}{\partial \nu}(x_4, t_4) < 0$, which is impossible. If $x_4 \in \Omega$, the strong maximum principle implies $S(x, t) \equiv 0, \forall (x, t) \in \Omega \times (0, t_4]$, and hence, $\Lambda(x) \equiv 0$, which is impossible. This proves (4.15).

The S -equation of (2.1) and (3.19) imply $\frac{\partial S}{\partial t} \geq D_S \Delta S + [\Lambda]_m - (a_1[\hat{\beta}_1]_M \mathbf{M}_\infty + [d_1]_M)S$. According to Lemma 3.2 and comparison principle, one can obtain (4.16). \square

Lemma 4.6. *Let $u_0 = (S_0, I_0, B_0)^T \in \mathbb{X}^+$. If $I_0 \not\equiv 0$ or $B_0 \not\equiv 0$, then*

$$I(x, t; u_0) > 0 \text{ and } B(x, t; u_0) > 0, \forall (x, t) \in \bar{\Omega} \times (0, \infty). \tag{4.17}$$

Proof. If $I_0(x) \not\equiv 0$, we consider

$$\begin{cases} \frac{\partial \bar{I}}{\partial t} = D_I \Delta \bar{I} - d(x)\bar{I}, & (x, t) \in \Omega \times (0, \infty), \\ \frac{\partial \bar{I}}{\partial \nu} = 0, & (x, t) \in \partial\Omega \times (0, \infty), \\ \bar{I}(x, 0) = I(x, 0) = I_0, & x \in \Omega. \end{cases}$$

It follows from [46, Lemma 1.26] that $\bar{I} > 0, \forall (x, t) \in \bar{\Omega} \times (0, \infty)$. By the comparison principle, $I(x, t) \geq \bar{I}(x, t) > 0, \forall (x, t) \in \bar{\Omega} \times (0, \infty)$. By the B -equation of (2.1),

$$B = B_0(x)e^{-\delta(x)t} + \int_0^t \beta_2(I(x, s), x)I(x, s)e^{-\delta(x)(t-s)} ds. \tag{4.18}$$

Hence, $B > 0, \forall (x, t) \in \bar{\Omega} \times (0, \infty)$. Thus, (4.17) holds.

If $B_0 \not\equiv 0$, we can obtain $B \geq (\neq)0, \forall t > 0$ by using (4.18). Then $\beta_1(I, x)SB \geq (\neq)0$. According to

$$I = \mathcal{T}_2(t)I_0(x) + \int_0^t \mathcal{T}_2(t-s)\beta_1(I, x)SB ds,$$

one gets $I(x, t) > 0$ for $(x, t) \in \bar{\Omega} \times (0, \infty)$. With proof similar to (4.18), one can obtain $B(x, t) > 0$ for $(x, t) \in \bar{\Omega} \times (0, \infty)$. This proves (4.17). \square

Lemma 4.7. *Let the initial condition $u_0 \in \mathbb{X}^+$, and σ_1 is defined in (4.16). If there exists a $\sigma_2 > 0$ such that either $\liminf_{t \rightarrow \infty} I(x, t; u_0) \geq \sigma_2$ or $\liminf_{t \rightarrow \infty} B(x, t; u_0) \geq \sigma_2$ uniformly for $x \in \bar{\Omega}$, then there is a positive constant $\tilde{\sigma}_2$ satisfying*

$$\liminf_{t \rightarrow \infty} (S, I, B)(x, t; u_0) \geq (\tilde{\sigma}_2, \tilde{\sigma}_2, \tilde{\sigma}_2), \text{ uniformly for } x \in \bar{\Omega}. \tag{4.19}$$

Proof. For the case of $\liminf_{t \rightarrow \infty} I(x, t; u_0) \geq \sigma_2$. As established in Lemma 4.5, (4.19) holds for S . We can choose $t_5 > 0$ satisfying $I(x, t) \geq \sigma_2$ for $(x, t) \in \bar{\Omega} \times [t_5, \infty)$. According to the B -equation of (2.1), one can obtain

$$\frac{\partial B}{\partial t} \geq \sigma_2(a_2 - b_2)[\hat{\beta}_2]_m - [\delta]_M B, (x, t) \in \bar{\Omega} \times [t_5, \infty).$$

The comparison principle implies

$$\liminf_{t \rightarrow \infty} B(x, t) \geq \frac{\sigma_2(a_2 - b_2)[\hat{\beta}_2]_m}{[\delta]_M}, \text{ uniformly for } x \in \bar{\Omega}. \tag{4.20}$$

For the case of $\liminf_{t \rightarrow \infty} B(x, t; u_0) \geq \sigma_2$. By Lemma 4.5, there exists $t_6 > 0$ satisfying

$$S(x, t) \geq \sigma_1 \text{ and } B(x, t) \geq \sigma_2, \forall (x, t) \in \bar{\Omega} \times [t_6, \infty).$$

Therefore, I -equation of (2.1) fulfills

$$\begin{cases} \frac{\partial I}{\partial t} \geq D_I \Delta I + \sigma_1 \sigma_2 (a_1 - b_1) [\hat{\beta}_1]_m - [d]_M I, & (x, t) \in \Omega \times [t_6, \infty), \\ \frac{\partial I}{\partial t} = 0, & (x, t) \in \partial\Omega \times [t_6, \infty). \end{cases}$$

Then Lemma 3.2 together with the comparison principle implies

$$\liminf_{t \rightarrow \infty} I(x, t) \geq \frac{\sigma_1 \sigma_2 (a_1 - b_1) [\hat{\beta}_1]_m}{[d]_M}, \text{ uniformly for } x \in \bar{\Omega}.$$

Take $\tilde{\sigma}_2 = \min \left\{ \sigma_1, \sigma_2, \frac{\sigma_2 (a_2 - b_2) [\hat{\beta}_2]_m}{[\delta]_M}, \frac{\sigma_1 \sigma_2 (a_1 - b_1) [\hat{\beta}_1]_m}{[d]_M} \right\}$, then the proof is completed. \square

We apply the similar proof as in [51, Theorem 3] to define

$$\begin{aligned} \mathbb{X}_0 &:= \{ \phi = (\phi_1, \phi_2, \phi_3)^T \in \mathbb{X}^+ : \phi_2 \not\equiv 0 \}, \\ \partial\mathbb{X}_0 &:= \{ \phi = (\phi_1, \phi_2, \phi_3)^T \in \mathbb{X}^+ : \phi_2 \equiv 0 \} \end{aligned}$$

and

$$M_\partial := \{ \phi = (\phi_1, \phi_2, \phi_3)^T \in \partial\mathbb{X}_0 : \Upsilon(t)\phi \in \partial\mathbb{X}_0, \forall t \geq 0 \},$$

where $\Upsilon(t) : \mathbb{X}^+ \rightarrow \mathbb{X}^+$ represents the semiflow of model (2.1)–(2.3).

Theorem 4.8. *For $\mathfrak{R}_0 > 1$ and $u_0 = (S_0, I_0, B_0)^T \in \mathbb{X}^+$ with $I_0 \not\equiv 0$ or $B_0 \not\equiv 0$, there is $\sigma > 0$ satisfying*

$$\liminf_{t \rightarrow \infty} (S, I, B)(x, t; u_0) \geq (\sigma, \sigma, \sigma), \text{ uniformly for all } x \in \Omega. \tag{4.21}$$

Furthermore, model (2.1)–(2.3) exists at least one PSS in \mathbb{X}^+ .

Proof. We only demonstrate Theorem 4.8 for $I_0 \not\equiv 0$. By using the similar argument, we can obtain Theorem 4.8 for $B_0 \not\equiv 0$. Lemmas 4.5 and 4.6 imply that $\Upsilon(t)\mathbb{X}_0 \subseteq \mathbb{X}_0, \forall t \geq 0$. Then we will elucidate the subsequent two claims.

Claim 1. Denoted by $\omega(u_0)$ the ω -limit set for orbit $\{\Upsilon(t)u_0 : t \geq 0\}$, $u_0 \in \mathbb{X}^+$. Then $\omega(u_0) = \{E_0\}$ for all $u_0 \in M_\partial$.

As for $u_0 \in M_\partial$, one can get $\Upsilon(s)u_0 \in M_\partial$, hence $I \equiv 0, \forall t \geq 0$. By I -equation in (2.1), Lemma 4.5 and $a_1 > b_1 \geq 0$ imply

$$\beta_1(I, x)SB \equiv 0, \quad x \in \Omega,$$

then $B \equiv 0$. Further Lemma 3.2 implies $S \rightarrow S^P(x)$ as $t \rightarrow \infty$ uniformly for $x \in \bar{\Omega}$. Thus, $\cup_{u_0 \in M_\partial} \omega(u_0) = \{E_0\}$.

Claim 2. There is $\hat{\sigma} > 0$ satisfying

$$\limsup_{t \rightarrow \infty} \|\Upsilon(t)u_0 - E_0\|_{\mathbb{X}} \geq \hat{\sigma}, \quad \forall u_0 \in \mathbb{X}_0.$$

Suppose to the contrary that for any given $\hat{\sigma} > 0$, there is $u_0 \in \mathbb{X}_0$ satisfying

$$\limsup_{t \rightarrow \infty} \|\Upsilon(t)u_0 - E_0\|_{\mathbb{X}} < \hat{\sigma}.$$

Thus, we can choose a sufficiently large $\tilde{t} > 0$ such that

$$S^P(x) - \hat{\sigma} < S(x, t; u_0), \quad I(x, t; u_0) < \hat{\sigma} \text{ and } B(x, t; u_0) < \hat{\sigma}, \quad \forall (x, t) \in \bar{\Omega} \times [\tilde{t}, \infty).$$

The comparison principle implies

$$(I, B) \geq (\tilde{I}, \tilde{B}) \text{ on } \bar{\Omega} \times [\tilde{t}, \infty),$$

where (\tilde{I}, \tilde{B}) satisfies

$$\begin{cases} \left(\begin{array}{c} \frac{\partial \tilde{I}}{\partial \tilde{t}} \\ \frac{\partial \tilde{B}}{\partial \tilde{t}} \end{array} \right) = \mathcal{B}_{\hat{\sigma}} \left(\begin{array}{c} \tilde{I} \\ \tilde{B} \end{array} \right), & (x, t) \in \Omega \times [\tilde{t}, \infty), \\ \frac{\partial \tilde{I}}{\partial \vartheta} = 0, & (x, t) \in \partial\Omega \times [\tilde{t}, \infty), \\ I(x, 0) = \tilde{I}(x, 0) = I_0, \quad \tilde{B}(x, 0) = B(x, 0) = B_0, \quad x \in \Omega \end{cases} \tag{4.22}$$

and

$$\mathcal{B}_{\hat{\sigma}} = \begin{pmatrix} D_I \Delta - d(x) & \beta_1(\hat{\sigma}, x)(S^P(x) - \hat{\sigma}) \\ \beta_2(\hat{\sigma}, x) & -\delta_1(x) \end{pmatrix}.$$

Hence (I, B) represents an upper solution of (4.22). It follows from $\mathfrak{R}_0 > 1$ and Lemma 4.1 that $s(\mathcal{B}) > 0$. According to (ii) of Theorem 4.3, one can get that $s(\mathcal{B})$ is the principal eigenvalue of (4.10). Let $s(\mathcal{B}_{\hat{\sigma}})$ be the principal eigenvalue of

$$\begin{cases} \lambda \begin{pmatrix} \psi_2 \\ \psi_3 \end{pmatrix} = \mathcal{B}_{\hat{\sigma}} \begin{pmatrix} \psi_2 \\ \psi_3 \end{pmatrix}, & x \in \Omega, \\ \frac{\partial \psi_2}{\partial \vartheta} = 0, & x \in \partial\Omega, \\ \psi_2 \in C^2(\Omega, \mathbb{R}) \cap C^1(\bar{\Omega}, \mathbb{R}), \quad \psi_3 \in C(\bar{\Omega}, \mathbb{R}) \end{cases} \tag{4.23}$$

with a strongly positive eigenfunction $\psi_{\hat{\sigma}} = (\psi_2^{\hat{\sigma}}(x), \psi_3^{\hat{\sigma}}(x))$. By continuity of $s(\mathcal{B}_{\hat{\sigma}})$ in $\hat{\sigma} > 0$, we can select small enough $\hat{\sigma} > 0$ satisfying $s(\mathcal{B}_{\hat{\sigma}}) > 0$. With the help of Lemma 4.6, one can select small enough $\tilde{\zeta} > 0$ satisfying $(I, B)(x, \tilde{t}; u_0) \geq \tilde{\zeta} \psi_{\hat{\sigma}}$. It follows from the comparison principle that

$$(I, B)(x, t; u_0) \geq \tilde{\zeta} e^{s(\mathcal{B}_{\hat{\sigma}})(t-\tilde{t})} \psi_{\hat{\sigma}}, \quad (x, t) \in \bar{\Omega} \times [\tilde{t}, \infty).$$

By $s(\mathcal{B}_{\hat{\sigma}}) > 0$, the above result implies that $I(x, t; u_0)$ and $B(x, t; u_0)$ are unbounded, a contradiction. Hence Claim 2 is proved.

Let $\rho : \mathbb{X}^+ \rightarrow \mathbb{R}_+$ be a continuous function and such that $\rho(u_0) = \min_{x \in \bar{\Omega}} \{I_0\}$, $u_0 \in \mathbb{X}^+$. For $u_0 \in \mathbb{X}_0$ and $t > 0$, lemma 4.6 implies that if $\rho(u_0) > 0$ or $\rho(u_0) = 0$, then $\rho(\Upsilon(t)u_0) > 0$. Therefore, it follows from [51, 52] that ρ represents a generalized distance function associated with $\Upsilon(t) : \mathbb{X}^+ \rightarrow \mathbb{X}^+$. Let

$$W^s(E_0) := \left\{ u_0 \in \mathbb{X}^+ : \lim_{t \rightarrow \infty} \|\Upsilon(t)u_0 - E_0\|_{\mathbb{X}} = 0 \right\}$$

be the stable set of E_0 . The above results imply that $W^s(E_0) \cap \rho^{-1}(0, \infty) = \emptyset$. Moreover, there exists no cycle in $\partial\mathbb{X}_0$ from E_0 to E_0 . Lemma 3.4 implies that $\Upsilon(t)$ has a global compact attractor. According to [52, Theorem 1.3.2], we can choose a $\sigma_3 > 0$ satisfying

$$\min_{v_0 \in \omega(u_0)} \rho(v_0) > \sigma_3, \quad \forall u_0 \in \mathbb{X}_0.$$

Hence,

$$\liminf_{t \rightarrow \infty} I(x, t; u_0) \geq \sigma_3, \quad \forall u_0 \in \mathbb{X}_0, \quad x \in \bar{\Omega}.$$

Moreover, Lemma 4.7 implies that there is a σ satisfying (4.21). It follows from [53, Theorem 3.7 and Remark 3.10] that $\Upsilon(t) : \mathbb{X}^+ \rightarrow \mathbb{X}^+$ possesses a global attractor. By [53, Theorem 4.7], Lemmas 4.5 and 4.6, model (2.1)–(2.3) possesses at least a PSS in \mathbb{X}_0 . \square

5. The impact of dispersal rates

In this section, the emphasis is placed on examining the dependency of the PSS and \mathfrak{R}_0 of model (2.1)–(2.3) on the dispersal rates of subpopulations (susceptible/infected) in scenarios where cholera persists uniformly. We examine the extreme cases of human mobility, where the dispersal rates of subpopulations either sufficiently small or large. On the other hand, these conclusions also reveal the pivotal role of human behavior change in influencing the characteristics of the PSS.

It follows from Theorem 4.8 that if $\mathfrak{R}_0 > 1$, then model (2.1)–(2.3) exists a PSS which fulfills

$$\begin{cases} D_S \Delta S + \Lambda(x) - \beta_1(I, x)SB - d_1(x)S = 0, & x \in \Omega, \\ D_I \Delta I + \beta_1(I, x)SB - d(x)I = 0, & x \in \Omega, \\ \beta_2(I, x)I - \delta(x)B = 0, & x \in \Omega, \\ \frac{\partial S}{\partial \vartheta} = \frac{\partial I}{\partial \vartheta} = 0, & x \in \partial\Omega. \end{cases} \tag{5.1}$$

Obviously,

$$B = \frac{\beta_2(I, x)I}{\delta(x)}, \tag{5.2}$$

then (5.1) fulfills

$$\begin{cases} D_S \Delta S + \Lambda(x) - \frac{\beta_1(I, x)\beta_2(I, x)}{\delta(x)}SI - d_1(x)S = 0, & x \in \Omega, \\ D_I \Delta I + \frac{\beta_1(I, x)\beta_2(I, x)}{\delta(x)}SI - d(x)I = 0, & x \in \Omega, \\ \frac{\partial S}{\partial \vartheta} = \frac{\partial I}{\partial \vartheta} = 0, & x \in \partial\Omega. \end{cases} \tag{5.3}$$

For convenience, we denoted $\varpi^\sharp = \int_{\Omega} \varpi(x)dx/|\Omega|$, $\varpi(x) \in C(\bar{\Omega})$.

Lemma 5.1. (see [49]) *For $h \in L^\infty(\Omega)$ and $D > 0$, let the principal eigenvalue of*

$$\begin{cases} D\Delta\varphi + h\varphi = \eta\varphi, & x \in \Omega, \\ \frac{\partial\varphi}{\partial\vartheta} = 0, & x \in \partial\Omega \end{cases} \tag{5.4}$$

be $\eta_1(D, h(x))$. Then

(i) $\eta_1(D, h) = \sup \left\{ \int_{\Omega} (-D|\nabla\varphi|^2 + h\varphi^2)dx : \varphi \in H^1(\Omega) \text{ with } \int_{\Omega} \varphi^2 dx = 1 \right\}$, which is a continuous function of D and $h(x)$;

(ii) $\eta_1(D, h)$ is increase as h ;

(iii) $\eta_1(D, h)$ is decrease as D and satisfies

$$\lim_{D \rightarrow 0} \eta_1(D, h) = \max\{h(x) : x \in \bar{\Omega}\} \text{ and } \lim_{D \rightarrow \infty} \eta_1(D, h) = h^\sharp.$$

Applying the methods in [35,54], the subsequent two lemmas hold.

Lemma 5.2. *For*

$$\begin{cases} D_I \Delta I - d(x)I + \frac{\beta_1(I, x)\beta_2(I, x)}{\delta(x)} \frac{\Lambda(x)}{\frac{\beta_1(I, x)\beta_2(I, x)I}{\delta(x)} + d_1(x)} I = 0, & x \in \Omega, \\ \frac{\partial I}{\partial \vartheta} = 0, & x \in \partial\Omega, \end{cases} \tag{5.5}$$

the following results are valid:

- (i) When $\hat{h}(D_I) := \eta_1(D_I, \frac{a_1 a_2 \hat{\beta}_1(x) \hat{\beta}_2(x) \Lambda(x)}{d_1(x) \delta(x)} - d(x)) \leq 0$, (5.5) possesses no positive solution;
- (ii) When $\hat{h}(D_I) := \eta_1(D_I, \frac{a_1 a_2 \hat{\beta}_1(x) \hat{\beta}_2(x) \Lambda(x)}{d_1(x) \delta(x)} - d(x)) > 0$, (5.5) possesses a unique positive solution.

Proof. (i) We apply the converse assumption that (5.5) possesses a positive solution I . We multiply (5.5) by I and integrate over Ω , resulting in

$$-D_I \int_{\Omega} |\nabla I|^2 dx + \int_{\Omega} \left(\frac{\beta_1(I, x) \beta_2(I, x)}{\delta(x)} \frac{\Lambda(x)}{\frac{\beta_1(I, x) \beta_2(I, x) I}{\delta(x)} + d_1(x)} - d(x) \right) I^2 dx = 0,$$

which implies

$$-D_I \int_{\Omega} |\nabla I|^2 dx + \int_{\Omega} \left(\frac{a_1 a_2 \hat{\beta}_1(x) \hat{\beta}_2(x) \Lambda(x)}{\delta(x) d_1(x)} - d(x) \right) I^2 dx > 0. \tag{5.6}$$

By the variational formula and (5.6), we get

$$\hat{h}(D_I) \geq \left(-D_I \int_{\Omega} |\nabla I|^2 dx + \int_{\Omega} \left(\frac{a_1 a_2 \hat{\beta}_1(x) \hat{\beta}_2(x) \Lambda(x)}{\delta(x) d_1(x)} - d(x) \right) I^2 dx \right) / \int_{\Omega} I^2 dx > 0,$$

a contradiction. Therefore (5.5) does not possess positive solution when $\hat{h}(D_I) \leq 0$.

- (ii) For $\hat{h}(D_I) > 0$, define ϕ as a positive eigenvector of (5.4) associated with $\hat{h}(D_I)$. Let

$$f(I) = D_I \Delta I + \left(\frac{\beta_1(I, x) \beta_2(I, x)}{\delta(x)} \frac{\Lambda(x)}{\frac{\beta_1(I, x) \beta_2(I, x) I}{\delta(x)} + d_1(x)} - d(x) \right) I.$$

Let $\check{I} = \epsilon \phi$ and $\epsilon > 0$ be small enough, we get

$$\begin{aligned} f(\check{I}) &= \epsilon \left(D_I \Delta \phi + \left(\frac{\beta_1(\epsilon \phi, x) \beta_2(\epsilon \phi, x)}{\delta(x)} \frac{\Lambda(x)}{\frac{\beta_1(\epsilon \phi, x) \beta_2(\epsilon \phi, x) \epsilon \phi}{\delta(x)} + d_1(x)} - d(x) \right) \phi \right) \\ &= \epsilon \left(\hat{h}(D_I) + \Lambda(x) \left(\frac{\beta_1(\epsilon \phi, x) \beta_2(\epsilon \phi, x)}{\delta(x)} \frac{1}{\frac{\beta_1(\epsilon \phi, x) \beta_2(\epsilon \phi, x) \epsilon \phi}{\delta(x)} + d_1(x)} - \frac{a_1 a_2 \hat{\beta}_1(x) \hat{\beta}_2(x)}{d_1(x) \delta(x)} \right) \right) \phi > 0. \end{aligned}$$

Therefore \check{I} represents a lower solution of (5.5) for $\epsilon > 0$. Suppose $\hat{I} = \hat{M}$ and $\hat{M} > 0$ be a constant. According to $\beta_i(I, x) = (a_i - b_i(1 - \frac{M_i}{I + M_i})) \hat{\beta}_i(x)$, $i = 1, 2$, we have $f(\hat{I}) < 0$ when \hat{M} is large.

Therefore \hat{I} represents an upper solution of (5.5). Then it follows from the method of upper/lower solution that (5.5) possesses a positive solution in $[\check{I}, \hat{I}]$.

The following goal is to verify the uniqueness of the positive solution. We apply the converse assumption that (5.5) exists two positive solutions, denoted by I_1 and I_2 , fulfilling $I_1 \not\equiv I_2$. By selecting ϵ sufficiently small and \hat{M} sufficiently large, one can ensure $I_i \in [\check{I}, \hat{I}]$, $i = 1, 2$. We can identify a minimal solution I_m and a maximal solution I_M of (5.5) fulfilling $I_m \not\equiv I_M$ within $[\check{I}, \hat{I}]$. Due to $I_1 \not\equiv I_2$, $I_m \leq I_M$ with $I_m \not\equiv I_M$. According to the method of upper/lower solution, $I_m < I_M$. On the other hand, by multiplying (5.5) with $I = I_M$ by I_m and (5.5) with $I = I_m$ by I_M , respectively, then subtracting the results, one can get

$$0 = \int_{\Omega} I_m I_M \Lambda(x) (g(I_M) - g(I_m)) dx,$$

where

$$g(I) = \frac{\beta_1(I, x) \beta_2(I, x)}{\delta(x)} \frac{1}{\frac{\beta_1(I, x) \beta_2(I, x) I}{\delta(x)} + d_1(x)}.$$

It then follows from $a_i > b_i \geq 0, i = 1, 2$ that $g(I)$ decreases strictly as $I > 0$. This implies $I_M = I_m$, which is a contraction. Hence, $I_1 = I_2$. \square

Lemma 5.3. For

$$\begin{cases} D_I \Delta I - d(x)I + \frac{\beta_1(I, x)\beta_2(I, x)I}{\delta(x)} \frac{\Lambda^\#}{\left(\frac{\beta_1(I)\beta_2(I)I}{\delta}\right)^\# + d_1^\#} = 0, & x \in \Omega, \\ \frac{\partial I}{\partial \nu} = 0, & x \in \partial\Omega, \end{cases} \tag{5.7}$$

the following results are valid:

- (i) When $\hat{h}(D_I) := \eta_1(D_I, \frac{a_1 a_2 \hat{\beta}_1(x)\hat{\beta}_2(x)\Lambda^\#}{\delta(x)d_1^\#} - d(x)) \leq 0$, (5.7) possesses no positive solution;
- (ii) When $\hat{h}(D_I) := \eta_1(D_I, \frac{a_1 a_2 \hat{\beta}_1(x)\hat{\beta}_2(x)\Lambda^\#}{\delta(x)d_1^\#} - d(x)) > 0$, (5.7) possesses a positive solution.

Proof. (i) For $\hat{h}(D_I) \leq 0$, we apply the converse assumption that (5.7) possesses a positive solution I . We multiply (5.7) by I and integrate over Ω , resulting in

$$-D_I \int_{\Omega} |\nabla I|^2 dx + \int_{\Omega} \left(\frac{\beta_1(I, x)\beta_2(I, x)}{\delta(x)} \frac{\Lambda^\#}{\left(\frac{\beta_1(I)\beta_2(I)I}{\delta}\right)^\# + d_1^\#} - d(x) \right) I^2 dx = 0,$$

which implies

$$-D_I \int_{\Omega} |\nabla I|^2 dx + \int_{\Omega} \left(\frac{a_1 a_2 \hat{\beta}_1(x)\hat{\beta}_2(x)\Lambda^\#}{\delta(x)d_1^\#} - d(x) \right) I^2 dx > 0. \tag{5.8}$$

By the variational formula and (5.8), we get

$$\hat{h}(D_I) \geq \left(-D_I \int_{\Omega} |\nabla I|^2 dx + \int_{\Omega} \left(\frac{a_1 a_2 \hat{\beta}_1(x)\hat{\beta}_2(x)\Lambda^\#}{\delta(x)d_1^\#} - d(x) \right) I^2 dx \right) / \int_{\Omega} I^2 dx > 0,$$

a contradiction. Therefore (5.7) does not possess positive solution when $\hat{h}(D_I) \leq 0$.

- (ii) For $\hat{h}(D_I) > 0$, define ϕ as a positive eigenvector of (5.4) associated with $\hat{h}(D_I)$. Let

$$f_1(I) = D_I \Delta I + \left(\frac{\beta_1(I, x)\beta_2(I, x)}{\delta(x)} \frac{\Lambda^\#}{\left(\frac{\beta_1(I)\beta_2(I)I}{\delta}\right)^\# + d_1^\#} - d(x) \right) I.$$

Let $\check{I} = \epsilon\phi$ and $\epsilon > 0$ be small enough, we get

$$\begin{aligned} f_1(\check{I}) &= \epsilon \left(D_I \Delta \phi + \left(\frac{\beta_1(\epsilon\phi, x)\beta_2(\epsilon\phi, x)}{\delta(x)} \frac{\Lambda^\#}{\left(\frac{\beta_1(\epsilon\phi)\beta_2(\epsilon\phi)\epsilon\phi}{\delta}\right)^\# + d_1^\#} - d(x) \right) \phi \right) \\ &= \epsilon \left(\hat{h}(D_I) + \Lambda^\# \left(\frac{\beta_1(\epsilon\phi, x)\beta_2(\epsilon\phi, x)}{\delta(x)} \frac{1}{\left(\frac{\beta_1(\epsilon\phi)\beta_2(\epsilon\phi)\epsilon\phi}{\delta}\right)^\# + d_1^\#} - \frac{a_1 a_2 \hat{\beta}_1(x)\hat{\beta}_2(x)}{\delta(x)d_1^\#} \right) \phi \right) > 0. \end{aligned}$$

Therefore \check{I} represents a lower solution of (5.7) for $\epsilon > 0$. Suppose $\hat{I} = \hat{M}$ and $\hat{M} > 0$ be a positive constant. According to $\beta_i(I, x) = (a_i - b_i(1 - \frac{M_i}{I + M_i}))\hat{\beta}_i(x)$, $i = 1, 2$, we have $f_1(\hat{I}) < 0$ when \hat{M} is large. Therefore \hat{I} represents an upper solution of (5.7). Then it follows from the method of upper/lower solution that (5.7) possesses a positive solution in $[\check{I}, \hat{I}]$. \square

5.1. Asymptotic profiles of the positive steady states and human behavior change

In certain scenarios, disease control strategies be designed to selectively target a particular subgroup within the population, leaving the other subgroup to move either unrestrictedly, or slowly, or rapidly. This underscores that a comprehensive understanding of the asymptotic profiles of the PSS would contribute to obtaining more precise information regarding the dynamics of cholera transmission. In this subsection, we set $D_I > 0$ as a constant and examine the behavior of the PSS as D_S toward small or large values.

Theorem 5.4. *For fixed $D_I > 0$, the following results are valid:*

- (i) *When $h(D_I) < 0$, then there exists $D_1 > 0$ such that (5.1) does not possess positive solution other than $(S^P(x), 0, 0)$ for $D_S < D_1$;*
- (ii) *When $h(D_I) > 0$, then there exists $D_2 > 0$ such that (5.1) possesses a positive solution (S, I, B) for $D_S < D_2$. Furthermore,*

$$(S, I, B) \rightarrow (S^{**}, I^{**}, B^{**}) = \left(\frac{\Lambda(x)}{\frac{\beta_1(I^{**},x)\beta_2(I^{**},x)I^{**}}{\delta(x)} + d_1(x)}, I^{**}, \frac{\beta_2(I^{**},x)I^{**}}{\delta(x)} \right), \text{ as } D_S \rightarrow 0, \tag{5.9}$$

where I^{**} be the unique positive solution of model (5.5). Moreover, If $a = a_i, b = b_i$ and $M = M_i$ for $i = 1, 2, I^{**}$ is decreasing in b and increasing in M .

Proof. (i) Obviously, $(S^P(x), 0, 0)$ is the positive solution of (5.1). If $D_S \rightarrow 0$, it follows that $S^P(x) \rightarrow \frac{\Lambda(x)}{d_1(x)}$. Thus,

$$\eta_1(D_I, \frac{a_1 a_2 \hat{\beta}_1(x) \hat{\beta}_2(x) S^P(x)}{\delta(x)} - d(x)) \rightarrow \eta_1(D_I, \frac{a_1 a_2 \hat{\beta}_1(x) \hat{\beta}_2(x) \Lambda(x)}{d_1(x) \delta(x)} - d(x)) = h(D_I). \tag{5.10}$$

By Theorem 4.3 (i), $\mathfrak{R}_0 - 1$ has the same sign as η_1 . If $h(D_I) < 0$, we can choose a $D_1 > 0$ such that $\mathfrak{R}_0 < 1$ for $D_S < D_1$. It follows from (5.2) and I equation of (5.3) that neither I nor B -equation of (5.3) possesses a positive solution when $D_S < D_1$.

- (ii) When $h(D_I) > 0$, according Theorem 4.3 (i), we can choose a $D_2 > 0$ such that $\mathfrak{R}_0 > 1$ for $D_S < D_2$. Therefore, Theorem 4.8 implies that (5.3) possesses a positive solution (S, I, B) for $D_S < D_2$.

The next goal is to verify the convergence of (S, I, B) . According to (5.3), we get

$$\begin{cases} -D_S \Delta S \leq \Lambda(x) - d_1(x)S, & x \in \Omega, \\ \frac{\partial S}{\partial \nu} = 0, & x \in \partial\Omega. \end{cases} \tag{5.11}$$

It follows from the maximum principle that

$$\|S\|_\infty \leq \bar{C}_1 := \frac{[\Lambda]_M}{[d_1]_m}, \quad \forall x \in \bar{\Omega}, \quad D_S > 0.$$

By the elliptic estimate, one can obtain

$$\|I\|_{W^{2,p}(\Omega)} \leq \bar{C}_2, \quad \forall x \in \Omega, \quad D_S > 0.$$

Combining methods from [18, Theorem 4.2], for $p > n$, we can select a sequence D_{S_k} with $D_{S_k} \rightarrow 0$ such that the positive solution (S_k, I_k) of (5.3) fulfills $(S_k, I_k) \rightarrow (S^{**}, I^{**})$ weakly in $(L^p(\Omega), W^{2,p}(\Omega))$ and $I_k \rightarrow I^{**}$ strongly in $C(\bar{\Omega})$ when $k \rightarrow \infty$. Then (5.3) implies that

$$S^{**} = \frac{\Lambda(x)}{\frac{\beta_1(I^{**},x)\beta_2(I^{**},x)I^{**}}{\delta(x)} + d_1(x)}. \tag{5.12}$$

Therefore, $S^{**}(x) > 0$. It follows from Lemma 5.2 that $I^{**}(x) = 0$ or $I^{**}(x) > 0$. Next, we claim that $I^{**}(x) > 0$. In fact, if $I^{**}(x) = 0$, then $S^{**}(x) = \frac{\Lambda(x)}{d_1(x)}$. Let $\bar{I}_k = \frac{I_k}{\|I_k\|_\infty}$ for all k . Then $\|\bar{I}_k\|_\infty = 1$ and \bar{I}_k

fulfills

$$\begin{cases} D_I \Delta \bar{I}_k - d(x) \bar{I}_k + \frac{\beta_1(I_k, x) \beta_2(I_k, x) \bar{I}_k}{\delta(x)} \frac{\Lambda(x)}{\frac{\beta_1(I_k, x) \beta_2(I_k, x) I_k}{\delta(x)} + d_1(x)} = 0, & x \in \Omega, \\ \frac{\partial \bar{I}_k}{\partial \vartheta} = 0, & x \in \partial\Omega. \end{cases} \tag{5.13}$$

According to L^p theory of elliptic equations, \bar{I}_k is uniformly bounded in $W^{2,p}(\Omega)$. Therefore, we can select a subsequence satisfying $\bar{I}_k \rightarrow \bar{I}^{**}$ weakly in $W^{2,p}(\Omega)$ as $k \rightarrow \infty$, where \bar{I}^{**} fulfills

$$\begin{cases} D_I \Delta \bar{I}^{**} - d(x) \bar{I}^{**} + \frac{a_1 a_2 \hat{\beta}_1(x) \hat{\beta}_2(x) \bar{I}^{**}}{\delta(x)} \frac{\Lambda(x)}{d_1(x)} = 0, & x \in \Omega, \\ \frac{\partial \bar{I}^{**}}{\partial \vartheta} = 0, & x \in \partial\Omega. \end{cases} \tag{5.14}$$

Recall that $\bar{I}_k > 0$ and $\|\bar{I}_k\|_\infty = 1$, thus,

$$\hat{h}(D_I) = \eta_1 \left(D_I, \frac{a_1 a_2 \hat{\beta}_1(x) \hat{\beta}_2(x) \Lambda(x)}{d_1(x) \delta(x)} - d(x) \right) = 0, \tag{5.15}$$

a contradiction with $\hat{h}(D_I) > 0$. Therefore, we obtain $I^{**}(\cdot) \neq 0$. Then (5.2) implies

$$B \rightarrow B^{**} = \frac{\beta_2(I^{**}, x) I^{**}}{\delta(x)} \text{ as } D_S \rightarrow 0. \tag{5.16}$$

To prove the monotonicity of I^{**} with respect to b and M , we rewrite (5.5) as follows:

$$\begin{cases} -D_I \Delta I^{**} + d(x) I^{**} = g(x, b, M, I^{**}) I^{**}, & x \in \Omega, \\ \frac{\partial I^{**}}{\partial \vartheta} = 0, & x \in \partial\Omega, \end{cases} \tag{5.17}$$

where

$$g(x, b, M, I^{**}) = \frac{(a - b \frac{I^{**}}{I^{**} + M})^2 \hat{\beta}_1(x) \hat{\beta}_2(x) \Lambda(x)}{(a - b \frac{I^{**}}{I^{**} + M})^2 \hat{\beta}_1(x) \hat{\beta}_2(x) I^{**} + d_1(x) \delta(x)}.$$

It is easy to obtain that $g(x, b, M, I^{**})$ is decreasing in b . Suppose $\bar{b} > b$, then $I_{\bar{b}}^{**}$ satisfies:

$$\begin{cases} -D_I \Delta I_{\bar{b}}^{**} + d(x) I_{\bar{b}}^{**} = g(x, \bar{b}, M, I_{\bar{b}}^{**}) I_{\bar{b}}^{**} < g(x, b, M, I_{\bar{b}}^{**}) I_{\bar{b}}^{**}, & x \in \Omega, \\ \frac{\partial I_{\bar{b}}^{**}}{\partial \vartheta} = 0, & x \in \partial\Omega, \end{cases}$$

which implies that $I_{\bar{b}}^{**}$ is a lower solution of (5.17). According to the proof of Lemma 5.2 (ii), one can get that the constant $\hat{M} > 0$ be an upper solution of (5.17) and $I^{**} \geq I_{\bar{b}}^{**}$.

It is easy to obtain that $g(x, b, M, I^{**})$ is increasing in M . Suppose $M > \bar{M}$, then $I_{\bar{M}}^{**}$ satisfies:

$$\begin{cases} -D_I \Delta I_{\bar{M}}^{**} + d(x) I_{\bar{M}}^{**} = g(x, b, \bar{M}, I_{\bar{M}}^{**}) I_{\bar{M}}^{**} < g(x, b, M, I_{\bar{M}}^{**}) I_{\bar{M}}^{**}, & x \in \Omega, \\ \frac{\partial I_{\bar{M}}^{**}}{\partial \vartheta} = 0, & x \in \partial\Omega, \end{cases}$$

which implies that $I_{\bar{M}}^{**}$ is a lower solution of (5.17). According to the proof of Lemma 5.2 (ii), one can get that the constant $\hat{M} > 0$ be an upper solution of (5.17) and $I^{**} \geq I_{\bar{M}}^{**}$. Theorem 5.4 holds. \square

For fixed D_I , we also investigate the behavior of the PSS when D_S becomes sufficiently large.

Theorem 5.5. *For fixed $D_I > 0$, the following results are valid:*

- (i) *When $\hat{h}(D_I) < 0$, then there exists $D_3 > 0$ such that (5.1) does not possess positive solution other than $(S^P(x), 0, 0)$ for $D_S > D_3$;*

(ii) When $\hat{h}(D_I) > 0$, then there exists $D_4 > 0$ such that (5.1) possesses a positive solution (S, I, B) for $D_S > D_4$. Moreover,

$$(S, I, B) \rightarrow (S^\infty, I^\infty, B^\infty) = \left(\frac{\Lambda^\sharp}{(\beta_1(I^\infty)\beta_2(I^\infty)I^\infty)^\sharp + d_1^\sharp}, I^\infty, \frac{\beta_2(I^\infty, x)I^\infty}{\delta(x)} \right), \text{ as } D_S \rightarrow \infty, \tag{5.18}$$

where I^∞ be the positive solution of (5.7).

Proof. (i) Apparently, $(S^P(x), 0, 0)$ is the positive solution of (5.1). If $D_S \rightarrow \infty$, it follows that $S^P(x) \rightarrow \frac{\Lambda^\sharp}{d_1^\sharp}$. Thus,

$$\eta_1(D_I, \frac{a_1 a_2 \hat{\beta}_1(x) \hat{\beta}_2(x) S^P(x)}{\delta(x)} - d(x)) \rightarrow \eta_1(D_I, \frac{a_1 a_2 \hat{\beta}_1(x) \hat{\beta}_2(x) \Lambda^\sharp}{d_1^\sharp \delta(x)} - d(x)) = \hat{h}(D_I). \tag{5.19}$$

By (i) of Theorem 4.3, $\mathfrak{R}_0 - 1$ has the same sign as η_1 . If $\hat{h}(D_I) < 0$, there is a $D_3 > 0$ such that $\mathfrak{R}_0 < 1$ for $D_S > D_3$. By a similar argument as (i) of Theorem 5.4, Lemma 5.3 implies that neither I nor B -equation of (5.3) possesses a positive solution when $D_S > D_3$.

(ii) when $\hat{h}(D_I) > 0$, according to Theorem 4.3 (i), we can choose a $D_4 > 0$ such that $\mathfrak{R}_0 > 1$ for $D_S > D_4$. Therefore, Theorem 4.8 implies that (5.3) possesses a positive solution (S, I, B) for $D_S > D_4$.

The next goal is to verify the convergence of (S, I, B) . By the similar processes in Theorem 5.4 (ii), we can select a sequence D_{S_k} with $D_{S_k} \rightarrow \infty$ such that the positive solution (S_k, I_k) of (5.3) fulfills $(S_k, I_k) \rightarrow (S^\infty, I^\infty)$ weakly in $(W^{2,p}(\Omega), W^{2,p}(\Omega))$ as $k \rightarrow \infty$. If $D_{S_k} \rightarrow \infty$, one can obtain $\Delta S^\infty = 0$. Thus, S^∞ is a constant. Then we integrate the S -equation of (5.3) to get

$$S^\infty = \frac{\Lambda^\sharp}{(\beta_1(I^\infty)\beta_2(I^\infty)I^\infty)^\sharp + d_1^\sharp}. \tag{5.20}$$

By the similar processes in Theorem 5.4, one can obtain $I^\infty \neq 0$ and

$$B \rightarrow B^\infty = \frac{\beta_2(I^\infty, x)I^\infty}{\delta(x)} \text{ as } D_S \rightarrow \infty. \tag{5.21}$$

This proof is completed. □

5.2. Asymptotic profiles of the basic reproduction number

This subsection will examine the impact of the human mobility on infection risk by discussing the asymptotic profiles of \mathfrak{R}_0 with small or large dispersal rates.

With the help of a singular perturbation argument as in the proof of [55, Lemma 3.2], we obtain $S^P(x) \rightarrow \frac{\Lambda(x)}{d_1(x)}$ when $D_S \rightarrow 0$. By applying 4.2 (i), one can establish the local basic reproduction number $\mathfrak{R}_0^l(x)$:

$$\mathfrak{R}_0^l(x) = \frac{a_1 a_2 \hat{\beta}_1(x) \hat{\beta}_2(x) \Lambda(x)}{d_1(x) d(x) \delta(x)}, \quad x \in \Omega. \tag{5.22}$$

Inspired by [49], one can get the low-risk region and the high-risk location: $\bar{\Omega}$ represents a low-risk region when $\mathfrak{R}_0^l(x) < 1, \forall x \in \bar{\Omega}$; x represents a high-risk location when $x \in \bar{\Omega}$ satisfies $\mathfrak{R}_0^l(x) > 1$.

Case 1. $(D_S, D_I) \rightarrow (0, 0)$. By (4.6), we have

$$\mathfrak{R}_1 := \lim_{(D_S, D_I) \rightarrow (0, 0)} \mathfrak{R}_0 = \max_{x \in \bar{\Omega}} \left\{ \frac{a_1 a_2 \hat{\beta}_1(x) \hat{\beta}_2(x) \Lambda(x)}{\delta(x) d_1(x) d(x)} \right\} = \max_{x \in \bar{\Omega}} \{ \mathfrak{R}_0^l(x) \}. \tag{5.23}$$

If $\bar{\Omega}$ is a low-risk region, $D_I > 0$ and $D_S \rightarrow 0$, then Theorem 4.2 (i) and (5.23) imply $\mathfrak{R}_0 < 1$. Thus, within the low-risk region $\bar{\Omega}$, our result indicates that cholera may potentially be eradicated by merely restricting the mobility of susceptible individuals.

If there exists high-risk location, then (5.23) implies $\mathfrak{R}_1 > 1$. Consequently, our result indicates that limiting human mobility alone is not sufficient to eliminate cholera if $\bar{\Omega}$ has high-risk location.

Case 2. $(D_S, D_I) \rightarrow (0, \infty)$. By (4.7), we have

$$\mathfrak{R}_2 := \lim_{(D_S, D_I) \rightarrow (0, \infty)} \mathfrak{R}_0 = \frac{\int_{\Omega} \left(\frac{a_1 a_2 \hat{\beta}_1(x) \hat{\beta}_2(x) \Lambda(x)}{\delta(x) d_1(x)} \right) dx}{\int_{\Omega} d(x) dx}. \tag{5.24}$$

If $\bar{\Omega}$ is a low-risk region, it follows from Theorem 4.2 (i) that $\mathfrak{R}_2 < 1$. By a similar arguments in Case 1, within the low-risk region $\bar{\Omega}$, the result implies that cholera may potentially be eradicated by merely restricting the mobility of susceptible individuals.

If there exists high-risk location, and $(d(\mathfrak{R}'_0 - 1))^{\#} < 0$, then Theorem 4.2 (iv) implies that we can select a $\hat{D}_I > 0$ satisfying $\mathfrak{R}_0 > 1$ for $D_I < \hat{D}_I$ and $\mathfrak{R}_0 < 1$ for $D_I > \hat{D}_I$. Obviously, $(d(\mathfrak{R}'_0 - 1))^{\#} < 0$ implies $\mathfrak{R}_2 < 1$. Consequently, our result indicates that even though $\bar{\Omega}$ has high-risk locations, at the same time, the average infection risk is small enough ($(d(\mathfrak{R}'_0 - 1))^{\#} < 0$), we can decrease the infection risk via accelerating the mobility of infected individuals when the mobility of susceptible individuals is small enough.

Apparently, $\mathfrak{R}_2 < \mathfrak{R}_1$, which suggests that when imposing restrictions the mobility of susceptible individuals, the rapid mobility of infected individuals reduces infection risk. This aligns with Theorem 4.2 (i).

On the other hand, recall that $S^P(x) \rightarrow \frac{\Lambda^{\#}}{d_1^{\#}}$ when $D_S \rightarrow \infty$. By applying Theorem 4.2 (i), one can establish the local basic reproduction number $\mathfrak{R}_0^L(x)$:

$$\mathfrak{R}_0^L(x) = \frac{a_1 a_2 \hat{\beta}_1(x) \hat{\beta}_2(x) \Lambda^{\#}}{d_1^{\#} d(x) \delta(x)}, \quad x \in \bar{\Omega}. \tag{5.25}$$

Similarly, we can get the low-risk region and the high-risk location with respect to $\mathfrak{R}_0^L(x)$: $\bar{\Omega}$ represents a low-risk region when $\mathfrak{R}_0^L(x) < 1, \forall x \in \bar{\Omega}$; x represents a high-risk location when $x \in \bar{\Omega}$ satisfies $\mathfrak{R}_0^L(x) > 1$.

Case 3. $(D_S, D_I) \rightarrow (\infty, 0)$. By (4.6), we have

$$\mathfrak{R}_3 := \lim_{(D_S, D_I) \rightarrow (\infty, 0)} \mathfrak{R}_0 = \max_{x \in \bar{\Omega}} \left\{ \frac{a_1 a_2 \hat{\beta}_1(x) \hat{\beta}_2(x) \Lambda^{\#}}{\delta(x) d_1^{\#} d(x)} \right\} = \max_{x \in \bar{\Omega}} \{ \mathfrak{R}_0^L(x) \}. \tag{5.26}$$

If $\bar{\Omega}$ is a low-risk region, then (5.26) and Theorem 4.2 (i) imply $\mathfrak{R}_0 < 1$. Hence, within the low-risk region $\bar{\Omega}$, the result indicates that cholera may potentially be eradicated when the susceptible individuals move at a rapid pace.

If there exists high-risk location, then (5.26) implies that $\mathfrak{R}_3 > 1$. Consequently, our result suggests that when $\bar{\Omega}$ has high-risk location, increasing the mobility of the susceptible individuals may enhance the cholera risk.

According to Case 1 and Case 3, we obtain that accelerating the mobility of susceptible individuals will enhance the risk of transmission for cholera when $\mathfrak{R}_1 < \mathfrak{R}_3$, while speeding up the mobility of susceptible individuals will decrease the infection risk when $\mathfrak{R}_1 > \mathfrak{R}_3$.

Case 4. $(D_S, D_I) \rightarrow (\infty, \infty)$. By (4.7), we have

$$\mathfrak{R}_4 := \lim_{(D_S, D_I) \rightarrow (\infty, \infty)} \mathfrak{R}_0 = \frac{\int_{\Omega} \left(\frac{a_1 a_2 \hat{\beta}_1(x) \hat{\beta}_2(x) \Lambda^{\#}}{\delta(x) d_1^{\#}} \right) dx}{\int_{\Omega} d(x) dx}. \tag{5.27}$$

If $\bar{\Omega}$ is a low-risk region, then (5.27) implies that $\mathfrak{R}_4 < 1$. By a similar arguments in Case 3, within the low-risk region $\bar{\Omega}$, the result indicates that cholera may potentially be eradicated if the susceptible individuals move at a rapid pace.

If there exists high-risk location, and $(d(\mathfrak{R}_0^L - 1))^\sharp < 0$, then Theorem 4.2(iv) implies that we can select a $\hat{D}_I > 0$ satisfying $\mathfrak{R}_0 > 1$ for $D_I < \hat{D}_I$ and $\mathfrak{R}_0 < 1$ for $D_I > \hat{D}_I$. Obviously, $(d(\mathfrak{R}_0^L - 1))^\sharp < 0$ implies $\mathfrak{R}_4 < 1$. Consequently, our result suggests that even though $\bar{\Omega}$ exists high-risk location, at the same time, the average infection risk is small enough $((d(\mathfrak{R}_0^L - 1))^\sharp < 0)$, we can decrease the disease via accelerating the mobility of infected individuals when the mobility of susceptible individuals is sufficiently large.

According to Case 1 and Case 4, we obtain that accelerating the mobility of individuals will enhance the risk of transmission for cholera when $\mathfrak{R}_1 < \mathfrak{R}_4$, while accelerating the mobility of individuals will decrease the risk of transmission for cholera when $\mathfrak{R}_1 > \mathfrak{R}_4$.

6. Numerical simulations

This section aims to employ numerical simulations to examine the impact of environmental heterogeneity and human behavior changes on the transmission of cholera. Specifically, our investigation focuses on understanding how alterations in human behavior, human mobility, and spatial heterogeneity influence both the risk of disease and the final epidemic size.

Within the field of epidemiology, considerable attention is given to the concepts of infection risk and the final epidemic size. The infection risk is directly linked to the basic reproduction number (\mathfrak{R}_0). Generally, an epidemic is expected to die out when $\mathfrak{R}_0 < 1$, while it becomes endemic when $\mathfrak{R}_0 > 1$. However, it is worth noting that for endemic situations where $\mathfrak{R}_0 > 1$, the computation of the total infection becomes unfeasible as it tends toward infinity.

To address this issue, we introduce the notation

$$H_I := \int_{\Omega} \tilde{I} dx$$

to quantify the final epidemic size, where $\tilde{I} \geq 0$ denotes the steady state solution of I -equation of (5.1). The definition given here is inspired by population size in ecology aspects [17, 24, 56].

The conclusions of this section are summarized as follows:

- (P1) Mitigating the spatial heterogeneity has the potential to eradicate cholera.
- (P2) Enhancing the mobility of infected individuals may make cholera extinct. For infection risk, the optimal dispersal rate of susceptible individuals lies in an intermediate range. Nevertheless, a reduction in the mobility of susceptible individuals may result in a decrease in the final epidemic size. Hence reliance solely on infection risk proves inadequate for predicting the final epidemic size.
- (P3) Human behavior changes have the capacity not only to precipitate a significant reduction in the final density of infected individuals, but also to forestall the escalation in the density of infected individuals over time in specific locations. Within a specific range, the expeditious response of media and individuals to cholera may prove more efficacious in controlling the final epidemic size than the associated largest reduced rates caused by human behavior changes.

Throughout this section, we vary specific parameter values to investigate the risk of disease and the final epidemic size for cholera. Inspired by Wang et al. [6], we set $\Omega = (0, 1) \subset \mathbb{R}$, and assume $D_S = 1$, $D_I = 0.01$ to represent the impact of the disease on human mobility. Particularly, we set $\Lambda(x) = 1 + \frac{\cos \pi x}{100}$ and $\hat{\beta}_1(x) = \hat{\beta}_2(x) = 1 + 0.5 \cos(5\pi x)$ for $x \in [0, 1]$ to reflect the spatial heterogeneity arising from differing geographical locations.

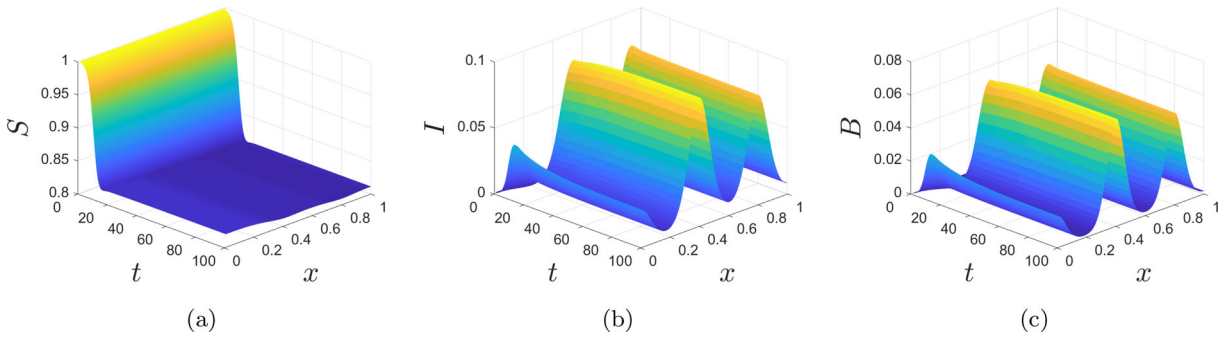


FIG. 1. Time evolution of **a** S , **b** I and **c** B of model (2.1)–(2.3) ($\mathfrak{R}_0 = 1.2479 > 1$)

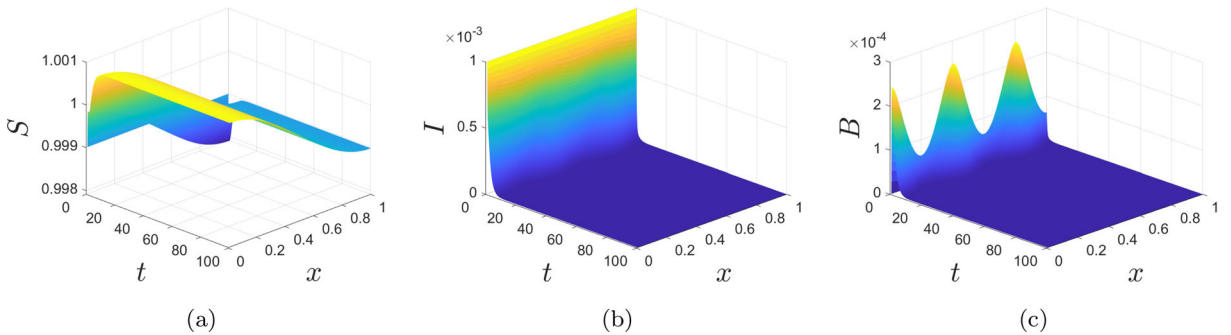


FIG. 2. Time evolution of **a** S , **b** I and **c** B of model (2.1)–(2.3) ($\mathfrak{R}_0 = 0.8320 < 1$)

6.1. \mathfrak{R}_0 and long-term behaviors

This subsection focuses on the simulations of model (2.1)–(2.3) for disease persistence and extinction, which align with Theorems 4.8 and 4.4. With

$$d_1 = 1, d = 5, \delta = 4, a_1 = 8.72, a_2 = 1.80, b_1 = 0.8a_1, b_2 = 0.8a_2, M_1 = M_2 = 10$$

and

$$S_0(x) = 0.999, I_0(x) = 0.001, B_0(x) = 0, x \in [0, 1],$$

we have $\mathfrak{R}_0 = 1.2479 > 1$, and Fig. 1 illustrates the uniform persistence of (2.1)–(2.3) and existence of the PSS. This result aligns with Theorem 4.8.

In fact, the control of cholera heavily relies on water sanitation and hygiene measures, as discussed by [57], ensuring access to safe water sources is particularly crucial in this regard. For instance, if we can enhance the mortality rate of *V. cholerae* in water reservoirs from the current value of $\delta = 4$ to $\delta = 6$ through methods like boiling water or treating it with chlorine-based products or household bleach, we find that $\mathfrak{R}_0 = 0.8320 < 1$. As shown in Fig. 2, the solution converges to the infection-free steady state (IFSS) over time. This finding aligns with the conclusion of Theorem 4.4.

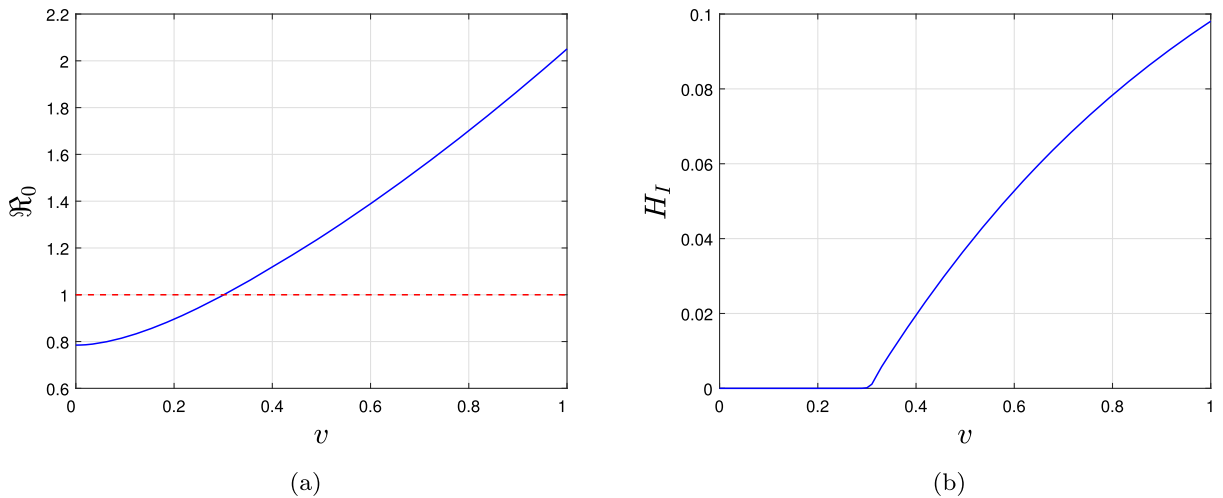


FIG. 3. **a** Sensitivity of \mathfrak{R}_0 to spatial heterogeneity v . **b** The final epidemic size H_I of system (2.1)–(2.3) with respect to v

6.2. Effects of spatial heterogeneity and dispersal rates

Let $v \in (0, 1)$ represent the spatial heterogeneity of the transmission rate from the environment to individuals and the shedding rate of the pathogen by infected individuals. By altering v , we can elucidate the effect of spatial heterogeneity on both the infection risk and the final epidemic size. Set

$$\hat{\beta}_1(x) = \hat{\beta}_2(x) = 1 + v \cos(5\pi x), \quad x \in [0, 1],$$

and the values of other parameters are consistent with Fig. 1. Figure 3a shows that \mathfrak{R}_0 increases monotonically with the increase of v . Figure 3b illustrates that H_I increases monotonically as v increases when endemic is established. These findings suggest that spatial heterogeneity may potentiate the infection risk and the final epidemic size.

On the other hand, let $D_I \in (0, 0.1)$ denote the dispersal rate of infected individuals, and the values of other parameters are consistent with Fig. 1. We investigate the impact of the dispersal rate of infected individuals on cholera by varying D_I . Figure 4a illustrates that \mathfrak{R}_0 increases monotonically with the increase of D_I . Figure 4b shows that H_I decreases monotonically as D_I increases when endemic is established. Thus, the mobility of infected individuals may decrease the infection risk and the final epidemic size.

Moreover, let $D_S \in (0, 10)$ denote the dispersal rate of susceptible individuals, the values of other parameters are consistent with Fig. 1. We investigate the impact of the dispersal rate of susceptible individuals on cholera by varying D_S . Figure 5a illustrates that \mathfrak{R}_0 decreases and subsequently increases as D_S increases. Thus, the effect of the mobility of susceptible individuals on the infection risk \mathfrak{R}_0 is complex, and the proper dispersal rate of susceptible individuals may minimize the risk of infection. Figure 5b shows that H_I monotonically increases as D_S increases. Therefore, decreasing the mobility of susceptible individuals may decrease the final epidemic size. Furthermore, by combining Fig. 5, we find that as D_S increases, the portion corresponding to the monotonic decrease of \mathfrak{R}_0 is accompanied by a monotonic increase in H_I . This indicates that infection risk alone is insufficient to predict the final epidemic size.

Remark 6.1. In fact, for the SIS model established in [24], numerical simulations exist to show that larger \mathfrak{R}_0 may not imply larger H_I . The corresponding theoretical result for a similar problem can be found in [56, 58]. However, we note that these numerical examples may not represent general results.

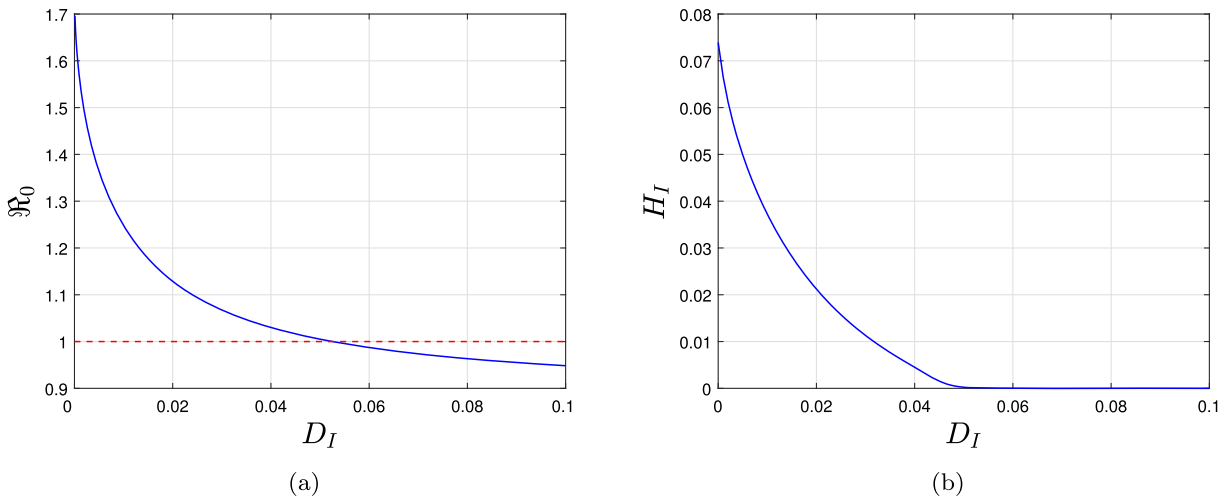


FIG. 4. **a** Sensitivity of \mathfrak{R}_0 to the dispersal rate of infected individuals D_I . **b** The final epidemic size H_I of system (2.1)–(2.3) with respect to D_I

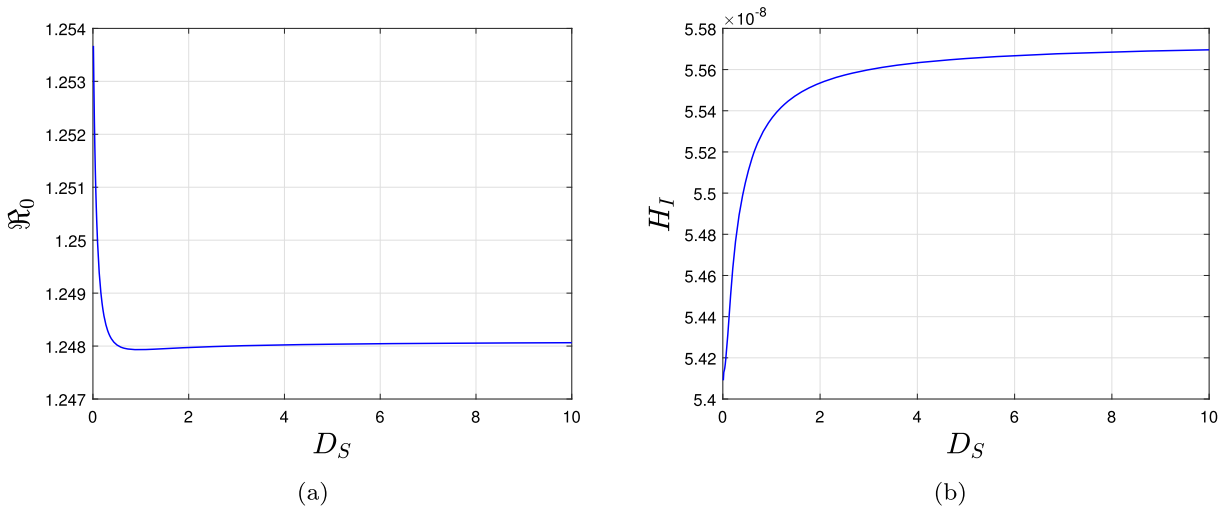


FIG. 5. **a** Sensitivity of \mathfrak{R}_0 to the dispersal rate of susceptible individuals D_S . **b** The final epidemic size H_I of system (2.1)–(2.3) with respect to D_S

6.3. Effect of human behavior changes

Now we study the influence of human behavior changes on the spread of cholera by varying locations (x), the associated largest reduced rates (b_1, b_2) caused by human behavior changes, or the response rates (M_1, M_2) of media and individuals to cholera. Specifically, we consider the locations $x = 0.2, x = 0.4$ and $x = 0.6$, respectively. Figure 6 illustrates how human behavior changes affect the transmission of cholera by analyzing the population density of infected individuals at different locations. The curves in blue, red, and green represent the densities of infected individuals under different scenarios: no behavior changes ($b_1 = b_2 = 0$), minor behavior changes ($b_i = 0.8a_i, M_i = 10, 1 \leq i \leq 2$), and significant behavior changes

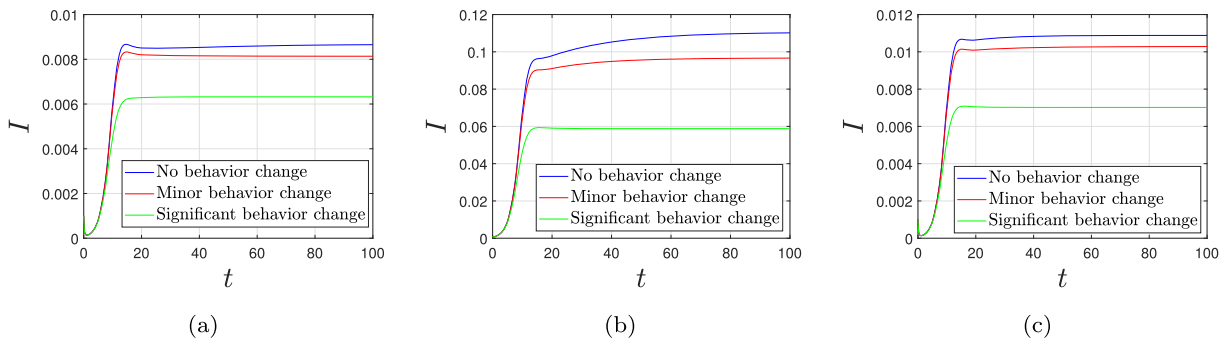


FIG. 6. Impacts of human behavior on cholera transmission at location **a** $x = 0.2$, **b** $x = 0.4$ and **c** $x = 0.6$

($b_i = 0.8a_i, M_i = 5, 1 \leq i \leq 2$), respectively. Moreover, Fig. 6b shows that the blue curve increases as time progresses, while the green curve decreases. These findings suggest that introducing human behavioral changes can be an effective strategy for controlling cholera transmission. Such changes can not only prevent the increase in the density of infected individuals over time in certain locations but also lead to a substantial decrease in the overall density of infected individuals. However, it is important to note that cholera cannot be eradicated solely by changing human behavior.

Furthermore, we investigate the influence of the associated largest reduced rates (b_1, b_2) caused by human behavior changes and the response rates (M_1, M_2) of media and individuals to cholera on the final epidemic size by varying b_i, M_i ($i = 1, 2$). Notice from (4.5) that these parameters do not impact \mathcal{R}_0 . We set $M_1 = M_2 := M$ and vary M within the range of $[0, 20]$. The other parameters are the same as those in Fig. 1. Figure 7a demonstrates that for $\mathcal{R}_0 > 1$, the epidemic size increases dramatically with M within a specific range. However, beyond this range, further increases in M have minimal effect on the final epidemic size. This suggests that the response rates of media and individuals to cholera can obviously influence the outbreak of cholera at the early stage. Similarly, we set $b_i = ba_i, 1 \leq i \leq 2$ for $b \in [0, 1]$ and keep the other parameters the same as in Fig. 1. Figure 7b shows that for $\mathcal{R}_0 > 1$, the final epidemic size decreases with b . This indicates that the associated largest reduced rates caused by human behavior changes may have an inverse relationship with the final epidemic size. Moreover, our results reveal that the effect of M on the final epidemic size H_I is greater than the effect of b within a specific range, suggesting that the rapid response of media and individuals to cholera may be more effective in controlling the final epidemic size within that range.

7. Discussion

Cholera possesses the capacity for swift spread over vast geographical regions, resulting in considerable mortality rates. There exists the potential for mathematical modeling to unravel the dynamics of cholera transmission and provide pragmatic recommendations for disease prevention. Several cholera models incorporating factors relevant to the disease have been formulated [6, 9, 21, 22, 38, 59]. However, the concurrent investigation of human behavior change, distinct human mobilities and spatial heterogeneity within a degenerate cholera model seems to be lacking in previous studies. In this paper, we extend the degenerate reaction-diffusion model [18] by incorporating the influence of human behavior change, i.e., the transmission rate and shedding rate of pathogen depend on the density of the infected individuals. The principal theoretical results presented in Sect. 3 include the well-posedness of the model by employing some estimates to address challenges associated with different dispersal rates and establish the existence of a global attractor for the degenerate equation by employing the κ -contraction condition.

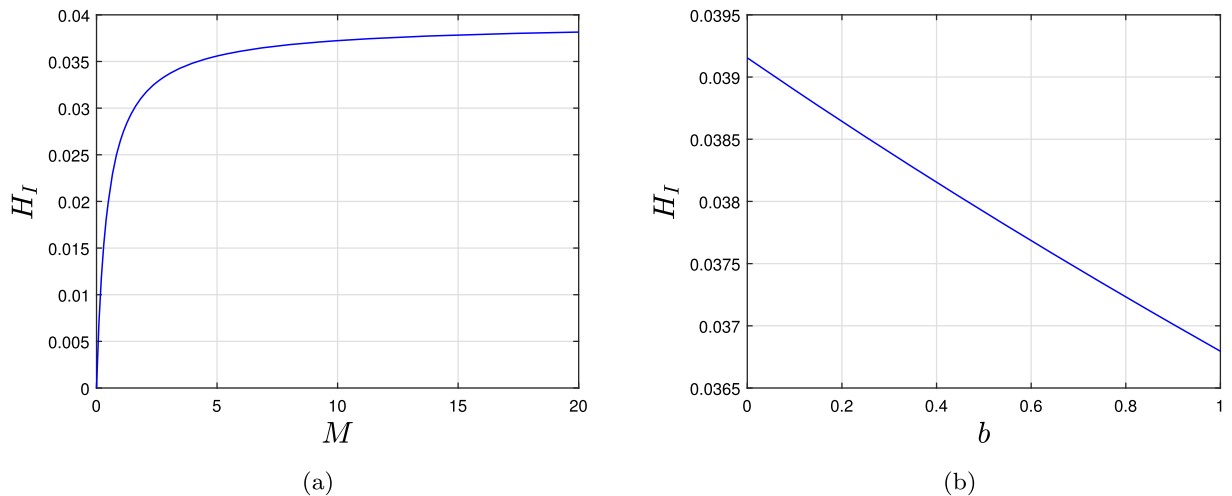


FIG. 7. The final epidemic size H_I of system (2.1)–(2.3) with respect to **a** the media and individuals respond to the epidemics M , **b** the largest reduced rate associated with behavior change in human hosts b

The basic reproduction number (\mathfrak{R}_0) is introduced in Sect. 4, and it is proven to serve as a threshold parameter for the extinction and persistence of epidemic. Specifically, when $\mathfrak{R}_0 < 1$, the infection-free steady state (IFSS) is globally asymptotically stable; while for $\mathfrak{R}_0 > 1$, the system exhibits uniform persistence and a positive steady state (PSS) exists. We observe that \mathfrak{R}_0 is independent of the associated largest reduced rates (b_1, b_2) caused by human behavior changes and the response rates (M_1, M_2) of media and individuals to cholera, but correlates with the dispersal rates. This indicates that the human behavior change does not influence the persistence of cholera, whereas human mobility does.

To conduct more information on the effects of human mobility, the asymptotic profiles of the PSS and \mathfrak{R}_0 are studied in Sect. 5. We derive the asymptotic profiles of the PSS for small or large dispersal rates of susceptible individuals, demonstrating that positive human behavior changes may reduce the final asymptotic profiles of PSS as small dispersal coefficients of susceptible individuals. It is noteworthy to highlight that there are two unresolved issues: the monotonicity of the final asymptotic profiles of PSS with respect to the coefficients associated with human behavior changes for large dispersal coefficients of susceptible individuals; the asymptotic profiles of the PSS for small and large values of infected individuals. Additionally, the asymptotic profiles of \mathfrak{R}_0 in relation to the extreme cases of human mobility are investigated. For regions with low cholera risk, it is found that cholera can potentially be eradicated by restricting the mobility of susceptible individuals. However, for regions with high cholera risk, restricting the mobility of infected individuals is not sufficient to eliminate cholera in certain cases. Instead, promoting the mobility of infected individuals can lead to cholera eradication when the average infection risk is sufficiently low. Furthermore, conditions are provided to demonstrate how human mobility can reduce the risk of disease transmission. These theoretical conclusions partially expand the insights into the asymptotic profiles of \mathfrak{R}_0 and the PSS for the cholera models incorporating human behavior changes [19, 20, 33].

Numerical simulations are conducted to further explore the influence of spatial heterogeneity, human mobility, and human behavior change on cholera transmission in Sect. 6. The simulations validate the theoretical conclusions and provide additional insights beyond the scope of the theoretical results. Spatial heterogeneity enhances the likelihood of cholera persistence, as depicted in Fig. 3. This observation implies that human behavior change and human mobility in spatially heterogeneous environments lead to interdependencies in the disease dynamics across distinct regions. The prevention and control of cholera

require a comprehensive approach rather than being an isolated concern for individual regions. The mobility of infected individuals may mitigate the spread of cholera, as shown in Fig. 4. Conversely, the mobility of susceptible individuals may exacerbate the transmission of cholera, as depicted in Fig. 5b. In epidemiology, the spatially homogeneous ordinary differential epidemic model commonly asserts that a higher basic reproduction number leads to a larger eventual infection size. Nevertheless, the applicability of \mathcal{R}_0 might be overemphasized. In the spatial epidemic model, the relationship between the basic reproduction number and the final epidemic size is non-monotonic, as illustrated in Fig. 5. This observation suggests that relying solely on the control of the basic reproduction number of cholera may not be efficacious. Furthermore, we ascertain that human behavior changes exert a positive impact on diminishing the final epidemic size, as depicted in Fig. 6. However, they fail to completely eradicate cholera alone. Furthermore, it is observed that the response rates (M) of media and individuals to cholera is more effective than the associated largest reduced rates (b) caused by human behavior changes in mitigating the final epidemic size to some extent, as shown in Fig. 7. Our results are consistent with the studies conducted by Fig. 3 in [19], Fig. 1 in [21] and further extend their contributions by studying the final epidemic size for cholera. These findings can potentially prevent cholera outbreaks at an early stage by identifying regions with heightened infection severity can optimize the allocation of available resources.

In this paper, we explore the transmission mechanism of cholera in the explicit incorporation of human behavior change, human mobility and spatial heterogeneity. To achieve this, we introduced several simplifying assumptions pertaining to the spread of cholera, such as the contact rate and shedding rate of individuals related to human behavior change. Actually, in regions characterized by a high prevalence of disease, susceptible individuals may actively seek to mitigate infection by leaving the area, thereby potentially decelerating the transmission of the epidemic [60–62]. We have also assumed that the density of *V. cholerae* in the polluted water is governed by the shedding rate of pathogen by infected individuals and the rate of natural mortality of *V. cholerae*. In fact, bacteria and bacteriophages maintain a predator–prey relationship. The ODE models [63,64] have been devised to integrate the interaction between bacteria and phage. Moreover, simulations suggest that spatial heterogeneity has the potential to enhance the epidemic risk and the final epidemic size. Future challenges include the development of theoretical results to elucidate the significance of spatial heterogeneity on recurrent cholera outbreaks.

Acknowledgements

The authors would like to thank the referees for their careful reading of the manuscript and constructive suggestions. Wenjing Wu and Shengqiang Liu’s research was partially supported by the National Natural Science Foundation of China (No. 12271401) and Natural Science Foundation of Tianjin, China (No. 22JCYBJC00080). Qianying Zhang’s research was partially supported by the National Natural Science Foundation of China (No. 12201457). Hao Wang’s research was partially supported by grants from the Natural Sciences and Engineering Research Council of Canada (Discovery Grant RGPIN-2020-03911 and Accelerator Grant RGPAS-2020-00090) and the Canada Research Chairs program (Tier 1 Canada Research Chair Award)

Author contributions Wenjing Wu and Shengqiang Liu wrote the main manuscript, Qianying Zhang revised the theoretical sections, and Hao Wang corrected the manuscript. All authors reviewed the manuscript.

Data availability No datasets were generated or analyzed during the current study.

Declarations

Conflict of interest The authors declare no Conflict of interest.

Publisher's Note Springer Nature remains neutral with regard to jurisdictional claims in published maps and institutional affiliations.

Springer Nature or its licensor (e.g. a society or other partner) holds exclusive rights to this article under a publishing agreement with the author(s) or other rightsholder(s); author self-archiving of the accepted manuscript version of this article is solely governed by the terms of such publishing agreement and applicable law.

References

- [1] Nelson, E.J., Harris, J.B., Morris, J.G., et al.: Cholera transmission: the host, pathogen and bacteriophage dynamics. *Nat. Rev. Microbiol.* **7**, 693–702 (2009)
- [2] Taylor, D.L., Kahawita, T.M., Cairncross, S., et al.: The impact of water, sanitation and hygiene interventions to control cholera: A systematic review. *PLoS ONE* **10**(8), e0135676 (2015)
- [3] Joh, R.I., Wang, H., Weiss, H., et al.: Dynamics of indirectly transmitted infectious diseases with immunological threshold. *Bull. Math. Biol.* **71**, 845–862 (2009)
- [4] Kong, J.D., Davis, W., Li, X., et al.: Stability and sensitivity analysis of the iSIR model for indirectly transmitted infectious diseases with immunological threshold. *SIAM J. Appl. Math.* **71**(5), 1418–1441 (2014)
- [5] Luo, J.H., Wang, J., Wang, H.: Seasonal forcing and exponential threshold incidence in cholera dynamics. *Discrete Contin. Dyn. Syst. Ser. B.* **22**(6), 2261–2290 (2017)
- [6] Wang, J.L., Wu, W.J., Kuniya, T.: Global threshold analysis on a diffusive host-pathogen model with hyperinfectivity and nonlinear incidence functions. *Math. Comput. Simul.* **203**, 767–802 (2023)
- [7] Hartley, D.M., Morris, J.G., Smith, D.L.: Hyperinfectivity: a critical element in the ability of *V. cholerae* to cause epidemics? *PLoS Med.* **3**(1), 63–69 (2006)
- [8] Mukandavire, Z., Liao, S., Wang, J., et al.: Estimating the reproductive numbers for the 2008–2009 cholera outbreaks in Zimbabwe. *Proc. Natl. Acad. Sci. U.S.A.* **108**(21), 8767–8772 (2011)
- [9] Wang, J.L., Wang, J.: Analysis of a reaction-diffusion cholera model with distinct dispersal rates in the human population. *J. Dyn. Diff. Equat.* **33**, 549–575 (2021)
- [10] Camach, A., Bouhenia, M., Alyusfi, R., et al.: Cholera epidemic in Yemen, 2016–18: an analysis of surveillance data. *Lancet Glob. Health.* **6**(6), 680–690 (2018)
- [11] Wang, J.: Mathematical models for cholera dynamics—A review. *Microorganisms* **10**(12), 2358 (2022)
- [12] Codeço, C.T.: Endemic and epidemic dynamics of cholera: the role of the aquatic reservoir. *BMC Infect. Dis.* **1**, 1 (2001)
- [13] Capasso, V., Paveri-Fontana, S.L.: A mathematical model for the 1973 cholera epidemic in the European Mediterranean region. *Rev. Epidemiol. Sante.* **27**(2), 121–132 (1979)
- [14] Hethcote, H.W., Ark, J.W.V.: Epidemiological models for heterogeneous populations: proportionate mixing, parameter estimation, and immunization programs. *Math. Biosci.* **84**(1), 85–118 (1987)
- [15] Hagenaars, T.J., Donnelly, C.A., Ferguson, N.M.: Spatial heterogeneity and the persistence of infectious diseases. *J. Theor. Biol.* **229**(3), 349–359 (2004)
- [16] Sun, G.Q., Li, L., Li, J., et al.: Impacts of climate change on vegetation pattern: mathematical modeling and data analysis. *Phys. Life Rev.* **43**, 239–270 (2022)
- [17] Lou, Y., Salako, R.B., Song, P.: Human mobility and disease prevalence. *J. Math. Biol.* **87**(1), 20 (2023)
- [18] Wu, Y., Zou, X.: Dynamics and profiles of a diffusive host-pathogen system with distinct dispersal rates. *J. Differ. Equ.* **264**, 4989–5024 (2018)
- [19] Wang, X.Y., Wu, R.W., Zhao, X.-Q.: A reaction-advection-diffusion model of cholera epidemics with seasonality and human behavior change. *J. Math. Biol.* **84**(5), 34 (2022)
- [20] Wang, W., Wu, G.X., Wang, X.A., et al.: Dynamics of a reaction-advection-diffusion model for cholera transmission with human behavior change. *J. Differ. Equ.* **373**, 176–215 (2023)
- [21] Wang, J.L., Wu, W.J., Kuniya, T.: Analysis of a degenerated reaction-diffusion cholera model with spatial heterogeneity and stabilized total humans. *Math. Comput. Simul.* **198**, 151–171 (2022)
- [22] Wang, J.L., Wu, X.Q.: Dynamics and profiles of a diffusive cholera model with bacterial hyperinfectivity and distinct dispersal rates. *J. Dyn. Diff. Equat.* **35**, 1205–1241 (2023)

- [23] Bauch, C.T., Galvani, A.P.: Social factors in epidemiology. *Science* **342**(6154), 47–49 (2013)
- [24] Song, P.F., Xiao, Y.N.: Analysis of a diffusive epidemic system with spatial heterogeneity and lag effect of media impact. *J. Math. Biol.* **85**(2), 17 (2022)
- [25] Li, W.J., Zhao, W.R., Cao, J.D., et al.: Dynamics of a linear source epidemic system with diffusion and media impact. *Z. Angew. Math. Phys.* **75**, 144 (2024)
- [26] Mukandavire, Z., Manangazira, P., Nyabadza, F., et al.: Stemming cholera tides in Zimbabwe through mass vaccination. *Int. J. Infect. Dis.* **96**, 222–227 (2020)
- [27] Dembinski, L., Stelmaszczyk-Emmel, A., Sznurkowska, K., et al.: Immunogenicity of cholera vaccination in children with inflammatory bowel disease. *Hum. Vaccin. Immunother.* **17**(8), 2586–2592 (2021)
- [28] Wang, X.Y., Gao, D.Z., Wang, J.: Influence of human behavior on cholera dynamics. *Math. Biosci.* **267**, 41–52 (2015)
- [29] Al-Arydah, M., Mwasu, A., Tchuente, J.M., et al.: Modeling cholera disease with education and chlorination. *J. Biol. Syst.* **21**(4), 1340007 (2013)
- [30] Anița, S., Capasso, V.: On the stabilization of reaction-diffusion systems modeling a class of man-environment epidemics: A review. *Math. Methods. Appl. Sci.* **33**(10), 1235–1244 (2010)
- [31] Capasso, V., Serio, G.: A generalization of the Kermack–McKendrick deterministic epidemic model. *Math. Biosci.* **42**(1–2), 43–61 (1978)
- [32] Carpenter, A.: Behavior in the time of cholera: evidence from the 2008–2009 cholera outbreak in Zimbabwe. *Lect. Notes Comput. Sci.* **8393**, 237–244 (2014)
- [33] Zhou, M.C., Wang, W., Fan, X.T., et al.: Threshold dynamics of a reaction-diffusion equation model for cholera transmission with waning vaccine-induced immunity and seasonality. *Z. Angew. Math. Phys.* **73**(5), 190 (2022)
- [34] Wang, W., Zhao, X.-Q.: Basic reproduction number for reaction-diffusion epidemic models. *SIAM J. Appl. Dyn. Syst.* **11**(4), 1652–1673 (2012)
- [35] Zha, Y.J., Jiang, W.H.: Global dynamics and asymptotic profiles for a degenerate dengue fever model in heterogeneous environment. *J. Differ. Equ.* **348**(5), 278–319 (2023)
- [36] Dwyer, G.: Density dependence and spatial structure in the dynamics of insect pathogens. *Am. Nat.* **143**(4), 533–562 (1994)
- [37] Wang, F.-B., Shi, J.P., Zou, X.F.: Dynamics of a host-pathogen system on a bounded spatial domain. *Commun. Pure. Appl. Anal.* **14**(6), 2535–2560 (2015)
- [38] Shu, H.Y., Ma, Z.W., Wang, H.: Diffusive host-pathogen model revisited: nonlocal infections, incubation period and spatial heterogeneity. *J. Math. Anal. Appl.* **516**(1), 126477 (2022)
- [39] Neilan, R.L.M., Schaefer, E., Gaff, H., et al.: Modeling optimal intervention strategies for cholera. *Bull. Math. Biol.* **72**(8), 2004–2018 (2010)
- [40] Wang, X.Y., Zhao, X.-Q., Wang, J.: A cholera epidemic model in a spatiotemporally heterogeneous environment. *J. Math. Anal. Appl.* **468**(2), 893–912 (2018)
- [41] Wang, L.W., Liu, Z.J., Zhang, X.G.: Global dynamics for an age-structured epidemic model with media impact and incomplete vaccination. *Nonlinear Anal. Real World Appl.* **32**, 136–158 (2016)
- [42] Smith, H.L.: *Monotone Dynamical Systems: an Introduction to the Theory of Competitive and Cooperative Systems*. American Mathematical Society, Providence, R.I (1995)
- [43] Martin, R.H., Smith, H.L.: *Abstract functional-differential equations and reaction-diffusion systems*. *Trans. Amer. Math. Soc.* **321**, 1–44 (1990)
- [44] Lou, Y.J., Zhao, X.-Q.: A reaction-diffusion malaria model with incubation period in the vector population. *J. Math. Biol.* **62**, 543–568 (2011)
- [45] Hale, J.K.: *Asymptotic Behavior of Dissipative Systems*. American Mathematical Society, Providence, R.I (1988)
- [46] Wang, M.X.: *Nonlinear Second Order Parabolic Equations*. CRC Press, Boca Raton (2021)
- [47] Thieme, H.R.: Spectral bound and reproduction number for infinite-dimensional population structure and time heterogeneity. *SIAM J. Appl. Math.* **70**(1), 188–211 (2009)
- [48] Du, Y.H.: Order structure and topological methods in nonlinear partial differential equations. In: *Maximum Principles and Applications*, vol 1. World Scientific, Singapore (2006)
- [49] Allen, L.J.S., Bolker, B.M., Lou, Y., et al.: Asymptotic profiles of the steady states for an SIS epidemic reaction-diffusion model. *Discrete Contin. Dyn. Syst. Ser. B* **21**(1), 1–20 (2008)
- [50] Nussbaum, R.D.: Eigenvectors of nonlinear positive operator and the linear Krein-Rutman theorem. In: *Fixed Point Theory, Lecture Notes in Mathematics*, vol 886. Springer, New York. pp. 309–331 (1981)
- [51] Smith, H.L., Zhao, X.-Q.: Robust persistence for semidynamical systems. *Nonlinear Anal.* **47**(9), 6169–6179 (2001)
- [52] Zhao, X.-Q.: *Dynamical Systems in Population Biology*, 2nd edn. Springer, New York (2017)
- [53] Magal, P., Zhao, X.-Q.: Global attractors and steady states for uniformly persistent dynamical systems. *SIAM J. Math. Anal.* **37**(1), 251–275 (2005)
- [54] Cantrell, R.S., Cosner, C.: *Spatial Ecology via Reaction-Diffusion Equations*. Wiley, Chichester, West Sussex (2003)
- [55] Peng, R., Shi, J., Wang, M.: On stationary patterns of a reaction-diffusion model with autocatalysis and saturation law. *Nonlinearity* **21**(7), 1471–1488 (2008)

- [56] Lou, Y.: On the effects of migration and spatial heterogeneity on single and multiple species. *J. Differ. Equ.* **223**(2), 400–426 (2006)
- [57] Lantagne, D., Yates, T.: Household water treatment and cholera control. *J. Infect. Dis.* **218**, 147–153 (2018)
- [58] Gao, D.Z.: How does dispersal affect the infection size? *SIAM J. Appl. Math.* **80**(5), 2144–2169 (2020)
- [59] Wang, X.Y., Wang, F.-B.: Impact of bacterial hyperinfectivity on cholera epidemics in a spatially heterogeneous environment. *J. Math. Anal. Appl.* **480**(2), 123407 (2019)
- [60] Cho, E., Kim, Y.-J.: Starvation driven diffusion as a survival strategy of biological organisms. *Bull. Math. Biol.* **75**, 845–870 (2013)
- [61] Wang, H., Wang, K., Kim, Y.-J.: Spatial segregation in reaction-diffusion epidemic models. *SIAM J. Appl. Math.* **82**(5), 1680–1709 (2022)
- [62] Wang, H., Salmani, Y.: Open problems in PDE models for knowledge-based animal movement via nonlocal perception and cognitive mapping. *J. Math. Biol.* **86**(5), 71 (2023)
- [63] Kong, J.D., Davis, W., Wang, H.: Dynamics of a cholera transmission model with immunological threshold and natural phage control in reservoir. *Bull. Math. Biol.* **76**, 2025–2051 (2014)
- [64] Botelho, C., Kong, J.D., Lucien, M.A.B., et al.: A mathematical model for Vibrio-phage interactions. *Math. Biosci. Eng.* **18**(3), 2688–2712 (2021)

Wenjing Wu, Qianying Zhang and Shengqiang Liu
School of Mathematical Sciences
Tiangong University
Tianjin 300387
China
e-mail: sqliu@tiangong.edu.cn

Wenjing Wu
e-mail: wjwu@tiangong.edu.cn

Qianying Zhang
e-mail: zhangqianying@tiangong.edu.cn

Hao Wang
Department of Mathematical and Statistical Sciences
University of Alberta
Edmonton ABT6G 2G1
Canada
e-mail: hao8@ualberta.ca

(Received: December 6, 2024; revised: April 9, 2025; accepted: April 14, 2025)